DETERMINATION OF THE EXIT VELOCITY OF THE JET NOZZLE OF A CO-FLOWING JET SENSOR

AMAL ZAKI BOUTROS

A DISSERTATION

IN THE

FACULTY OF ENGINEERING

Presented in partial fulfilment of the requirements for the Degree of MASTER OF ENGINEERING

at

CONCORDIA UNIVERSITY
Montreal, Canada

September, 1975

DETERMINATION OF THE EXIT VELOCITY OF THE JET NOZZLE OF A CO-FLOWING JET SENSOR

AMAL ZAKI BOUTROS

ABSTRACT

This work represents an attempt to determine the exit velocity of the jet nozzle in a co-flowing air velocity sensor, under different values of the supply pressure and in a zero free-stream velocity.

The sensor consists of a nozzle (0.023 in ID by 0.5 in. long) and receiver assembly which when placed in a free stream of unknown velocity can be used to measure that free-stream velocity. In a previous study [8] the jet spreading characteristics is predicted for different nozzle exit velocities. The present work is a theoretical and experimental investigation to determine the volume flow coefficient of the nozzle at different supply pressures. To determine the exit temperature, it is necessary to make an assumption regarding the flow process through the nozzle. Calculations are made for three cases; ideal flow, adiabatic flow and isothermal flow. The results are presented as plots of the volume discharge coefficient versus both the Reynold's number and the flow number. At choked flow conditions the flow coeffficients for isothermal and adiabatic flows differ by less than 2% at corresponding Reynold's numbers and flow numbers. Flow coefficient based on either definition can therefore be used within these limits of accuracy.

An attempt is made to calculate the pressure drop across the duct using the previously determined exit conditions and published values of entrance losses for fully developed laminar and turbulent flow. The

greatest deviation between calculated and actual pressure drops occurs in the transition region where there is little published information of the friction factor - Reynold's number relationship.

ACKNOWLEDGEMENTS

The author wishes to express sincere thanks to Professor M.P. duPlessis and Dr. Sui Lin for their valuable suggestions, supervision and guidance. She is also thankful for the contribution of Mr. M. Hashish particularly in the experimental work.

TABLE OF CONTENTS

TABLE OF CONTENTS (continued)

Page

LIST OF FIGURES

LIST OF TABLES

NOMENCLATURE

D	Inlet diameter of the duct
L	Length of the duct
A	Cross-sectional area
Q_{th}	Theoritical volume rate of flow at the exit of the nozzle
Q_{Exit}	Measured volume rate of flow at the exit conditions of the nozzle
C	Sonic velocity
C_D	Discharge coefficient
C_v	Specific heat at constant volume
C_p	Specific heat at constant pressure
C_q	Flow coefficient of the nozzle
M	Mach number
h_m	Minor losses
Re	Reynold's number based on diameter basis
K_{bend}	Resistance due to bend
D_h	Hydraulic diameter
p	Static pressure
f'	Friction coefficient
f	Friction factor
k	Specific heat ratio
R	Gas constant
ρ	Density
dA_w	Wetted wall area

NOMENCLATURE (continued)

g	Acceleration due to gravity
μ	Dynamic viscosity
w	Mass flow rate
k_L	Entrance loss coefficient
K	Entrance correction factor = $k_L + 1$
V	Mean velocity of the fluid
ν	Kinematic viscosity
T	Absolute temperature
τ_w	Shear stress due to wall
λ	Flow number
x	Axial coordinate

Prefixes: Δ Large increment

Subscripts:

$(\ )_1$	state at section 1
$(\ )_2$	state at section 2
$(\ )_o$	stagnation state
$(\ )^*$	state at which M = 1 for adiabatic flow
$(\ )^{*t}$	state at which $M = 1/\sqrt{k}$ in isothermal flow
$(\ )_s$	static
$(\ )_{Is}$	isentropic
$(\ )_{If}$	isothermal, frictionless
$(\ )_{th}$	theoretical
$(\ )_{Exit}$	state at the exit of the nozzle

CHAPTER I

INTRODUCTION

CHAPTER I

1.1 Introduction

Active fluid dynamic devices employing interaction of a free turbulent jet with the measured flow have some advantages over conventional passive devices used to measure the velocity of a fluid. Hot wires or film gauges are delicate and suffer from a lack of proportionality between measured velocity and output. Pitot tube square law output presents limitations on the measurement sensitivity at low velocities. Rotating devices provide an output proportional to the measured velocity, but tend to stall at lwo velocities.

The co-flowing sensor conceived, developed and tested at NRC [1,2] (Figs. 1 and 2) have a high sensitivity (0.03 in water / ft.s^{-1} in air) and anotably wide range (0 to 720 ft.s^{-1} in air). Further, it has the particularly desirable feature that the output receiver pressure varies linearly with the free stream velocity for certain ranges of jet and stream velocities.

The construction of the co-flowing sensor is simple and rugged; it permits measurement in ducts as small as 1 in. diameter or in unbounded flows.

The sensor consists of a turbulent-jet generating power nozzle and a receiver assembly which is placed in a free stream of which either the velocity or the density is known.

This work represents an attempt to determine the exit velocity of the jet nozzle in a co-flowing air velocity sensor, under different values of the supply pressure and in a zero free-stream velocity.

An attempt is also made to calculate the pressure drop across the nozzle using the previously calculated exit conditions.

1.2. Principle of Operation

The sensor operation is based on the mixing of the turbulent jet issuing from a power nozzle with a co-flowing stream; the resultant jet dynamic pressure is detected by a downstream co-axial receiver tube, where the nozzle to receiver distance is typically 14/d to 20/d. The intensity of mixing, in being dependent on the fluid shear stress between the jet and the measured stream, will be a unique function of the free stream velocity for a given jet velocity. In particular, at zero stream velocity, the shear stress and resultant mixing intensity will be maximum for a given nozzle supply pressure; thus the spreading rate of the turbulent free jet will be maximum and the resulting centerline dynamic pressure at the receiver will be minimum. Conversely, at free stream velocities equal to the jet velocity, the shear stress will be minimized for a given supply pressure; thus the spreading rate of the jet will be minimum and the resulting centerline dynamic pressure at the receiver will be substantially greater than for zero measured stream velocity. Figure 2 shows the details of the duct flow sensor dealt with in this study.

1.3 Summary of Prior Investigation

The development of a turbulent jet immersed in a parallel and co-flowing stream has been investigated by a number of authors on the basis of simplified [3] or extensive theoretical analysis [4] incorporating experimentally determined constants.

Previous work consisted of determining the performance characteristics of two experimental sensor configurations in a variable density wind tunnel to simulate both pipe and confined flow measurement applications [2]. Dimensional analysis coupled with experimental evaluation showed that the sensor sensitivity is directly proportional to measured flow static density, for a given geometry and supply pressure within defined broad operating limits.

Previous studies [5,6,7], have presented explicit and implicit numerical methods for the solution of jet flow in the near jet region. Recent work [8], presented a finite difference solution of the momentum equation to predict the velocity decay of an isothermal, turbulent, incompressible co-flowing jet in zero pressure gradient using the Pantakar-Spalding method [9] coupled with a simple mixing length turbulence model, previously developed for submerged jets [7]. The method requires that the conditions (velocity, pressure and temperature) of the free stream and power jet be known at the nozzle exit. The receiver pressure can then be calculated from the predicted velocity profiles at different distances from the nozzle.

The finite difference method requires that the starting velocity profile at the nozzle exit be known. The jet exit velocity profile cannot be conveniently measured experimentally. The main task of this study consists of predicting the jet nozzle exit velocity at different applied differential pressures.

1.4 Description of the Problem

The co-flowing jet sensor (Figs. 1 and 2) consists of a turbulent jet generating power nozzle coupled to a pressure supply p_s, a single receiver is located on the centerline of the nozzle connected to a suitable pressure measuring device, and the necessary mounting hardware for the nozzle and receiver. A static pressure tap, mounted on the cylindrical duct surface, permits the measurement of the pressure differential at the nozzle exit.

The nozzle of the ducted sensor used in this study consists of a 0.1 in. internal diameter by 2.0 in. long entrance tube brazed to a 0.023 in. internal diameter by 0.5 in. long exit nozzle as shown in Figure 3.

The task is to predict the velocity of the flow at the exit of the nozzle given the values of the pressure differential for the tube and nozzle assembly.

In the experimental investigation, the rate of flow, Q, was measured for different values of the pressure differential between the nozzle supply and the nozzle exit, ranging from 0.1 psi to 14 psi.

The nozzle exit velocity V_2 could be predicted if the temperature T_2 was known; although the ambiant temperature at the nozzle exit region is known, the jet exit temperature can differ from this value.

i. Approximate Classification of the Flow

a) In section 1, approximate calculations show that the Mach number is low (max. value = 0.03) and that the Reynold's number is very low (max. value at pressure differential value of about 14 psi = 3000). The flow is therefore subsonic, incompressible and laminar in this section.

b) In section 2, the Mach number exceeds 0.3 at low pressure differential and reaches 0.78 at about 14 psi. Reynold's number exceeds 3000. The flow is therefore in the compressible, turbulent region.

ii. Method of Analysis

a) Between sections 1 and 1' the flow is incompressible and laminar. For the fully developed flow, the Darcy-Weisbach equation can be applied:

$$\frac{\Delta P}{L} = \frac{f}{D}\,\frac{\rho V^2}{2}$$

where f is the fully developed friction factor. From the Moody equation $f = \frac{64}{Re_D}$ for laminar flow in smooth and rough pipes. Minor losses due to the 90 degree bend can be expressed for fully developed flow as follows: [13]

$$h_m = K_{bend}\,\frac{V^2}{2g}$$

where K_{bend} is the resistance due to the bend; its value depends on the ratio r/R where r is the radius of curvature, and R is the inside radius of the tube.

The total pressure drop in section 1 is then:

$$\Delta P_1 = (f \frac{L}{D} + K_{bend}) \frac{\rho V^2}{2}$$

b) The process from section 1' to 2 is more complicated and could be analyzed as adiabatic or isothermal with friction. The total length of this section is of 0.5 in., this means that $\frac{L}{D} = \frac{0.5}{0.023} = 21.7$. The entrance length for incompressible, turbulent flow is about 30 hydraulic diameters or less (about 20 to 25 for Reynold's number of 150,000 or higher). The entrance length depends on the entrance shape and on the Reynold's number. The flow in this part of the nozzle is laminar at low pressure differentials and turbulent at high supply pressures. The flow at 21.7 hydraulic diameters may not be fully developed particularly under laminar conditions, and losses due to entrance will be difficult to evaluate.

The losses from section 1 to 1' will be very small compared to that from section 1' to 2 (maximum of 0.2% of total losses).

Conclusion

Analytical prediction of the exit velocity of the nozzle is difficult; it requires a separate study of the compressible flow losses in the tube entrance section which may account for the largest portion of the total losses.

The more conventional approach is to express the losses in the form of discharge coefficients which are determined experimentally.

CHAPTER II

FLOW COEFFICIENT

CHAPTER II

FLOW COEFFICIENT

2.1 Definition of the Flow Coefficient

Following Shapiro [12], a nozzle flow coefficient is defined by

$$W_{actual} = C_q W_{th} \tag{2.1}$$

where W_{actual} = the actual nozzle mass rate of flow

C_q = the flow coefficient

W_{th} = the theoretical mass flow rate.

Equation (2.1) can also be written as

$$(\rho Q)_{actual} = C_q (\rho Q)_{th} \tag{2.2}$$

In this study, the objective is to determine the actual exit volume flow rate;

i.e. $$Q_{Exit} = C_q \frac{\rho_{th}}{\rho_{Exit}} Q_{th} \tag{2.3}$$

The temperature at the exit of the nozzle is unknown, its value depends on the thermodynamic process taking place across the nozzle. The actual thermodynamic process must be defined so that Q_{Exit}, ρ_{Exit} can be determined.

In the case of incompressible flow,

$$Q_{th} = Q_{Ideal}$$

and $$\rho_{th} = \rho_{Exit} = \text{constant}$$

Equation (2.3) becomes

$$Q_{Exit} = C_q Q_{Ideal} \tag{2.4}$$

In the case of adiabatic process,

$$Q_{th} = Q_{Is} \; , \quad \rho_{th} = \rho_{Is}$$

where Q_{Is} = Isentropic volume rate of flow at the exit of the nozzle.

ρ_{Is} = The density at the exit of the nozzle calculated from isentropic flow equations.

and $$Q_{Exit} = C_q \frac{\rho_{Is}}{\rho_{Exit}} \cdot Q_{Is} \tag{2.5}$$

or $$Q_{Exit} = C_q' \cdot Q_{Is} \tag{2.6}$$

where $$C_q' = C_q \cdot \frac{\rho_{Is}}{\rho_{Exit}} \tag{2.7}$$

$$C_q' = C_q \; , \quad \text{if } \rho_{Is} = \rho_{Exit} = \rho_{adiabatic} \tag{2.8}$$

If the flow is isothermal,

$$Q_{th} = (Q_{Isothermal})_{frictionless} = Q_{If}$$

and $$\rho_{th} = \rho_{If}$$

then $$Q_{Exit} = C_q \frac{\rho_{If}}{\rho_{Exit}} \cdot Q_{If} \tag{2.9}$$

or $$Q_{Exit} = C_q'' \; Q_{If} \tag{2.10}$$

where $$C_q'' = C_q \cdot \frac{\rho_{If}}{\rho_{Exit}} \tag{2.11}$$

$$C_q'' = C_q, \text{ if } \rho_{If} = \rho_{Exit} = \rho_{isothermal} \tag{2.12}$$

Since the actual process is neither adiabatic nor isothermal, the values of C_q, C_q' and C_q'' were calculated from equations (2.4, 2.6, 2.10). Q_{Exit} was obtained from the flow rates measured at the inlet different pressure ratios across the nozzle.

$$Q_{Exit}\ (\text{at } P_2 \text{ and } T_2) = Q_{measured}\ (\text{at } P_2 \text{ and } T_1) \cdot \frac{T_2}{T_1} \qquad (2.13)$$

The values of C_q, C_q' and C_q'' were obtained from equations (2.1), (2.6) and (2.10) using measured values of Q at approaximately 30 different pressure differentials.

In general, it is known that $C_q = f_n$ (Re, M); this relationship is studied for each of the assumed flow processes in the following section.

2.2 Experimental Determination of the Flow Coefficient of the Nozzle Assuming Incompressible Flow

Following the traditional method of describing flow through short-tube nozzles and orifices, the actual flow rate can be obtained from the equation:

$$Q_{Exit} = C_q Q_{Ideal}$$

where C_q is determined experimentally.

The energy equation for a fully developed, incompressible flow through the nozzle is:

$$p_1 + \frac{\rho V_1^2}{2} = p_2 + \frac{\rho V_2^2}{2}$$

$$p_1 - p_2 = \rho\left(\frac{V_2^2}{2} - \frac{V_1^2}{2}\right) \qquad (2.14)$$

Neglecting the kinetic energy at the entrance, the energy equation will reduce to:

$$\Delta p_s = \frac{\rho V_2^2}{2} \qquad (2.15)$$

where V_2 is the ideal velocity at the nozzle exit and Δp_s is the static pressure difference at the entrance and exit of the nozzle assembly.

Hence

$$V_2 = \sqrt{\frac{2\Delta p_s}{\rho}}$$

$$Q_{Ideal} = V_2 A_2$$

where A_2 is the nozzle exit cross-sectional area

$$Q_{Ideal} = A_2\sqrt{\frac{2\Delta p_s}{\rho}} \qquad (2.16)$$

Q_{actual} is measured using a rotameter with a metering float of 0.25 in. diameter (Fisher and Porter Company, precision base flowmeter tube no. FP - ¼ - 20 - G - 5).

Correction for metering pressure is accomplished using the rotameter charts, no correction is done for the temperature assuming that the temperature at the nozzle exit is ambiant.

$$Re = \frac{\rho_2\, Q_{Exit} \cdot D_2}{A_2\, \mu_2}$$

$$= \frac{\rho_2\, V_{2(Exit)} \cdot D_2}{\mu_2} \qquad (2.17)$$

The Flow Number [10]:

From equation (2.17), it is evident that the value of Reynold's number can only be determined if the actual mean velocity through the nozzle is available.

To avoid this difficulty, it seems convenient to represent the variation of the flow coefficient as a function of the flow number λ where

$$\lambda = D_2/\nu\sqrt{2(p_2 - p_1)/\rho_2} \qquad (2.18)$$

The flow number can be evaluated without prior knowledge of C_q and the flow coefficient can then be easily found from graphs of C_q and λ.

The results obtained experimentally in this work are given in Figure 5. The variation of the flow coefficient is plotted with both Reynold's number and the flow number.

The comparison of the results of this work (Fig. 5) and that obtained by Lichtarowicz et al. [11], (Fig. 8) shows that:

- the L/D ratio of this study is 20 whereas that of Lichtarowicz has a maximum of 10. No detailed comparison can therefore be made, even though the flow number ranges correspond in the range 10^3 and $1.1x10^4$. The L/D factor becomes less at flow numbers greater than 10^4.
- the values for C_q at flow numbers between 10^3 and $1.1x10^4$ are higher than the values obtained by Lichtarowicz et al. This is surprising since the trend in Figure 8 is for C_q to decrease with increasing L/D values.
- the values for C_q at flow numbers higher than $1.1x10^4$ are generally in the same range as those obtained by Lichtarowicz et al.

The following section investigates for the variation of the entrance coefficient at different values of Reynold's number. This investigation should permit to conclude whether or not the flow is fully developed across the nozzle.

2.3 Flow Coefficient Assuming the Flow Through the Nozzle is Adiabatic

The theoretical flow rate through the nozzle assembly is assumed to be isentropic. It is necessary to determine the inlet and outlet conditions so that the theoretical exit velocity can be calculated.

The supply pressure to the nozzle is measured, and the pressure at the exit of the nozzle is atmospheric. The temperature at the nozzle exit can then be found using isentropic flow equations. Mach numbers at section 1 and section 2 can be calculated using two simultaneous equations relating the supply and exit pressure and the cross-section area ratio.

a- Exit Temperature

The relations between pressure, temperature and density for an isentropic process of a perfect gas are:

$$\frac{P_2}{P_1} = (\frac{\rho_2}{\rho_1})^k \; ; \; \frac{T_2}{T_1} = (\frac{P_2}{P_1})^{\frac{k-1}{k}} \qquad (2.19)$$

The temperature at the nozzle exit is then given by the equation:

$$T_2 = T_1 \, (\frac{P_2}{P_1})^{\frac{k-1}{k}} \qquad (2.20)$$

and

$$\rho_2 = \rho_1 \, (\frac{T_2}{T_1})^{1/k-1} \qquad (2.21)$$

b- <u>Mach Number</u>

From the one dimensional, steady, isentropic flow equations of a perfect gas, we can write:

$$\frac{P_o}{P} = (1 + \frac{k-1}{2} M^2)^{k/k-1} \qquad (2.22)$$

Then

$$\frac{P_2}{P_1} = \frac{(1 + \frac{k-1}{2} M_1^2)^{k/k-1}}{(1 + \frac{k-1}{2} M_2^2)^{k/k-1}} \qquad (2.23)$$

$$(\frac{P_2}{P_1})^{\frac{k-1}{k}} = \frac{(1 + \frac{k-1}{2} M_1^2)}{(1 + \frac{k-1}{2} M_2^2)}$$

Hence, for air,

$$M_2 = \sqrt{\frac{1 + 0.2 \, M_1^2}{0.2 (\frac{P_2}{P_1})^{0.4/1.4}} - 5} \qquad (2.24)$$

We can also write:

$$\left(\frac{w}{A}\right)_{max} = \left(\frac{w}{A^*}\right) = \sqrt{\frac{k}{R}\left(\frac{2}{k+1}\right)^{\frac{k+1}{k-1}}} \cdot \frac{P_o}{\sqrt{T_o}} \qquad (2.25)$$

from which

$$\frac{A_1}{A_2} = \frac{M_2}{M_1}\left[\frac{\left(1+\frac{k-1}{2}\ M_1^{\,2}\right)}{\left(1+\frac{k-1}{2}\ M_2^{\,2}\right)}\right]^{\frac{k+1}{2(k-1)}} \qquad (2.26)$$

For air, this equation can be rearranged to yield

$$\frac{A_1\ M_1}{A_2(1+0.2\ M_1^{\,2})^3} = \frac{M_2}{(1+0.2\ M_2^{\,2})^3} \qquad (2.27)$$

Equations (2.24) and (2.27) can be solved simultaneously using iterative calculation. The value of M_1 is assumed, M_2 is then calculated from equation (2.24). The two terms (R.H.S. and L.H.S.) of equation (2.27) are then calculated and compared; the value of M_1 is changed and the calculation is repeated to finally obtain the equality of the two terms of equation (2.27). This method is applied to the different values of the supply pressure. The results of this procedure are represented in Table 1.

c- <u>Flow Coefficient of the Nozzle</u>

From equation (2.6)

$$Q_{Exit} = Q_{Is}\ C_q'$$

where $Q_{Is} = V_{Is} \cdot A_2 = M_2\ C_2\ A_2$

and $C_2 = \sqrt{k\ R\ T_2}$

Using equation (2.20) to replace T_2 by T_1 we get

$$C_2 = k\ R\ T_1\ (\frac{p_2}{p_1})^{\frac{k-1}{2k}}$$

The relation between the measured rate of flow and the actual rate of flow at the exit of the nozzle is given by the equation

$$Q_{Exit}\ (\text{at } p_2 \text{ and } T_2) = Q(\text{measured at } p_2 \text{ and } T_1) \cdot \frac{T_2}{T_1}$$

Hence

$$C_q = \frac{Q_{measured} \cdot T_2/T_1}{M_2\ A_2 \quad kRT_1} \cdot (\frac{p_2}{p_1})^{\frac{1-k}{2k}} \qquad (2.28)$$

$$Re_2 = \frac{Q_{Exit} \cdot \rho_2 \cdot D_2}{A_2 \cdot \mu_2} \text{ and } \lambda = \frac{\rho_2\ V_{Isent.} \cdot D_2}{\mu_2} \qquad (2.29)$$

where ρ_2 = the density of air at p_2 and T.

The assumption of an adiabatic process across the nozzle to calculate the flow rate leads to a variation of the flow coefficient as represented in Figure 6. It is interesting to note that, the curve obtained with Reynold's number agrees with the curve of incompressible flow up to a Mach number of 0.40; above this value the curve shows a deviation and approaches the form of Lichtarowicz [11] (Fig. 8)

The difference between the adiabatic flow process curve and the incompressible flow curve at high Mach number values (Fig. 7), reduces significantly when the flow number is used instead of Reynold's number.

2.4 Flow Coefficient Assuming Isothermal Flow Process

The flow can be assumed isothermal at low Mach numbers.

The Mach number at section 1 is assumed to be the same as determined in section 2.3, the inlet conditions being identical.

The temperature and pressure at sections 1 and 2 as well as the density at section 2 are known; the missing parameters necessary to determine the flow coefficient are the exit Mach number (M_2) and the density at section 1.

a- Mach Number

For isothermal process in a perfect gas, we can write:

$$M = V/C = V/\sqrt{kRT}$$

$$M^2 = V^2/kRT, \quad \text{and } T \text{ is constant}$$

at $M = 1/\sqrt{k}$, $V = V^{*t}$ [12,13]

where V^{*t} is the critical velocity where M attains the limiting value $1/\sqrt{k} = 0.85$ for air.

Therefore, $$\frac{M^2}{V^2} = \frac{1/k}{(V^{*t})^2}$$

from which $$\frac{V}{V^{*t}} = \sqrt{k}\ M \tag{2.30}$$

The perfect gas relation yields

$$\frac{p}{p^{*t}} = \frac{\rho}{\rho^{*t}} \quad \text{when } T \text{ is constant.}$$

From continuity:

$$\rho_1 V_1 A_1 = \rho_2 V_2 A_2$$

$$\frac{\rho_1 V_1}{\rho_2 V_2} = \frac{A_1}{A_2} \tag{2.31}$$

From equation (2.30)

$$\frac{V_1}{V_2} = \frac{M_1}{M_2}$$

From the perfect gas relation

$$\frac{p_1}{p_2} = \frac{\rho_1}{\rho_2}$$

Replacing in equation (2.31) for V_1/V_2 and p_1/p_2 we obtain

$$\frac{p_1 \; M_1}{p_2 \; M_2} = \frac{A_1}{A_2}$$

from which

$$M_2 = M_1 \cdot \frac{p_1}{p_2} \cdot \frac{A_2}{A_1} \tag{2.32}$$

b- <u>Flow Coefficient</u>

It is known from equation (2.10) that

$$C_q'' = Q_{Exit} \; / \; Q_{If}$$

where $Q_{Exit} = Q_{measured}$ (at T_1 and p_2)

Also, $Q_{If} \quad V_{If} \cdot A_2 \quad M_2C_2A_2$

where $C_2 = \sqrt{kRT_1}$

Hence

$$C_q = \frac{Q_{measured}}{M_2A_2\sqrt{kRT_1}}$$

$$Re_2 = \frac{Q_{Exit} \cdot \rho_2 \cdot D_2}{A_2 \cdot \mu_2}$$

and

$$\lambda = \frac{\rho_2 \, V_{If} \cdot D_2}{\mu_2}$$

The results obtained through the assumption of a compressible isothermal process are represented in Table 3 in the Appendix.

The variation of the flow coefficient with Reynold's number is shown in Figure 6 and the variation with the flow number is plotted in Figure 7.

Comparison of the curves plotted for compressible and incompressible flow processes (Figs. 6 and 7) shows that the flow can be treated as incompressible up to a flow number value of about 7000. At higher values of flow number, the flow is compressible and an intermediate process between adiabatic and isothermal processes may be considered. However, the adiabatic flow curve can be used with a maximum error of about 2% on the C_q value and of about 6% on the exit flow rate value considering the fact that a continuous isothermal flow process is limited by a maximum exit Mach number of 0.85, and that $Q_{Exit}(\text{adiabatic}) = Q_{Exit}(\text{isothermal}) \cdot \frac{T_2}{T_1}$.

CHAPTER III

PRESSURE DROP EVALUATION

CHAPTER III

PRESSURE DROP EVALUATION

To evaluate the pressure drop through the jet nozzle assembly, it is obvious that we can separate the problem into two parts: the pressure loss between section 1 and section 1' which is easy to evaluate and contribute by a negligible portion to the total loss, and the pressure drop between section 1' and 2 which represents the major part of the total drop. The evaluation of the losses between section 1' and 2 is complicated due to the sudden contraction at section 1'. Entrance losses must be considered and friction losses depend on the nature of the flow.

Moreover, the flow cannot be treated as incompressible when Mach number is higher than 0.3; this implies that different hypothesis must be considered to predict the thermodynamic process of the flow between section 1' and 2.

3.1 Losses Between Section 1 and Section 1'

The flow in section 1 can be treated as incompressible, steady and laminar; Mach number does not exceed 0.03 and the maximum Reynold's number is of about 3400 on tube diameter basis.

$$\text{Hence} \quad \Delta p_1 = \left(f \frac{L}{D} + k_{bend}\right) \frac{\rho V_1^2}{2}$$

where k_{bend} is the resistance due to the 90° bend; its value is expressed as an equivalent length in diameter [6], and

$$f = \frac{64}{Re_1}$$

$$\Delta p_1 = \left(\frac{64}{Re_1} \cdot \frac{L}{D} + k_{bend}\right) \frac{\rho V_1^2}{2}$$

where $\frac{L}{D} = \frac{2}{0.1} = 20$

3.2 Study of the Flow Between Sections 1' and 2

In general, the losses in a tube are calculated using coefficients whose values are based on fully developed flow conditions. It is of a great importance to determine if the flow, at the exit of the nozzle under study in this work, is fully developed.

Entrance Length:

When a fluid passes into a duct from a chamber of different cross-sectional area, its velocity profile undergoes a development in the course of the flow through the duct. The entrance length is the distance from the duct entrance necessary to achieve the balance between the pressure and viscous forces and to attain essentially fully developed conditions with unchanging velocity profile.

For practical purposes, it is usually sufficient to associate the entrance length with the distance from the entrance of the duct necessary to the pressure gradiant to approach to within 5 percent to the fully developed value [14].

It is also of practical use, to associate the entrance length to the distance along the axis where the centerline velocity reaches 99 percent of its fully developed value [15].

The pressure gradiant at the entrance of a tube generally becomes constant before the velocity profile; the entrance lengths based on the pressure gradiant stabilization are then shorter than those based on the velocity profile development [14].

The entrance length in a tube depends on Reynold's number, on the shape of the entrance, and on the nature of the flow.

At very high Reynold's number, the turbulent entrance length is only moderately affected by the magnitude of the Reynold's number, while at law Reynold's number, the entrance length is very sensitive to the magnitude of the Reynold's number.

The entrance lengths in laminar flow are longer than those in turbulent flow [16].

We use in this work the definition of the entrance length as the distance required to the centerline velocity to approach to 99 percent to the fully developed value.

The entrance length $(\frac{L}{D})_e$ for an incompressible, isothermal steady state laminar flow in a circular tube is related to the Reynold's number by the equation:

$$(\frac{L}{D})_e = \frac{0.72}{(0.04\ Re + 1)} + 0.061\ Re \qquad \text{after Chen [15]}$$

or

$$(\frac{L}{D})_e = \frac{0.60}{(0.035\ Re + 1)} + 0.056\ Re \qquad \text{after Friedman et al. [17]}$$

$$(\frac{L}{D})_e = 0.06\ Re \qquad \text{after Langhaar [18]}$$

where $(\frac{L}{D})_e$ is the dimensionless entrance length in pipe diameters.

In our case, the minimum value of Reynold's number at the laminar flow region, corresponds to an entrance length of about 38 pipe diameters. The nozzle dimensionless length is 21.7 nozzle diameters; it is then clear that the flow across the nozzle is not fully developed under the laminar regime.

3.3 Pressure Drop Between Sections 1' and 2

In calculating the pressure drop, it is convenient to use fully developed friction factors and to add a correction term to account for entrance effects. The pressure drop across the nozzle is then given by the equation:

$$p_1' - p_2 = \Delta p = (f \frac{L}{D_h} + K) \rho V_2^2 / 2 \qquad (3.1)$$

where D_h = the hydraulic diameter

= D for the circular tube

and K accounts for the acceleration of the fluid from rest (or V_1) and the development of the velocity profile, and the incremental dissipation in the entrance region relative to that in fully developed region.

K can also be defined as $K = 1 + k_L$ [14,16]

where k_L is the entrance loss coefficient.

The value of f, the friction factor, depends on the nature of the flow, laminar or turbulent, compressible or incompressible, adiabatic or isothermal.

a- Determination of the Value of K

The value of K depends on the nature of the flow; it is also a function of the position at the entrance region, but becomes constant in the fully developed flow regime.

At low values of Reynold's number, K is a function of the position at the entrance region, and varies with the magnitude of Reynold's number. The variation of K at low Reynold's number was investigated by Chen [15] and by Hornbeck [19]; the curves representing this variation are shown in Figure 9.

At very high Reynold's number, the entrance length is moderately affected by the magnitude of the Reynold's number; the value of K is then moderately affected.

From Chen [15] and Hornbeck [19] curves, it is obvious that the value of K is decreasing in the laminar flow regime as far as the Reynold's number is increasing at the exit of the nozzle.

The value of K for a fully developed incompressible flow has been determined by many researchers [14,16,18,20,21] and varies from 1.18 to 1.5. After Chen [15] $K_\infty = (1.20 + 38/Re)$ at low Reynold's number values, and after Olson [16] it has the value of 1.39 for a sudden contraction of $\frac{D_2}{D_1} = 0.2$.

At a fixed distance from the entrance, K decreases when Reynold's number increases at the laminar flow regime; it reaches a minimum value at the transition zone, then increases in the turbulent flow conditions to reach a constant value when the flow becomes fully developed [16,22].

The variation of the value of K is determined using equation 3.1

$$K = \left[\Delta p \;/\; \left(\frac{\rho V^2}{2}\right)\right] - f\,\frac{L}{D}$$

The value of f is obtained after the investigation of the flow. Four assumptions are considered:

1- The flow is steady, incompressible, isothermal and laminar.

2- The flow is steady, incompressible, isothermal and turbulent.

3- The flow is compressible and adiabatic with friction.

4- The flow is compressible and isothermal with friction.

b- Determination of the Friction Factor f

First Assumption:

Treating the flow as steady, incompressible, isothermal and laminar, we can obtain the value of the friction factor using Moody equation for smooth and rough pipes.

Hence $$f = \frac{64}{Re_2} \tag{3.2}$$

where $$Re_2 = \frac{\rho_2 V_2}{\mu_2} \text{ at } p_2 \text{ and } T_2 = T_1 \tag{3.3}$$

Second Assumption:

Assuming the flow to be steady, incompressible, isothermal and turbulent; the friction factor is obtained using Blasius law for smooth pipes. Then

$$f = 0.316 / Re_2^{1/4} \tag{3.4}$$

Third Assumption:

The determination of the friction factor for a compressible adiabatic flow with friction in a circular duct is more complicated; the gas is assumed to be perfect and the equations of adiabatic flow in constant area duct must be derived.

Definition of the Friction Coefficient

The friction coefficient is defined as the ratio of the wall shearing stress to the dynamic head of the stream.

Thus:

$$f' = \frac{\tau_w}{\rho V^2/2}$$

The friction factor used in Blasius relation or in Darcy-Weisbach equation is four times the friction coefficient. Thus,

$$f = 4 f' = \frac{4 \tau_w}{\rho V^2/2} \tag{3.5}$$

The hydraulic diameter D_h is defined as:

$$D_h = \frac{4 A}{dA_w/d_x} = 4 \frac{A}{dA_w} dx \tag{3.6}$$

it is four times the ratio of cross-sectional area to wetted perimeter; in the case of a circular tube, it is equal to the inlet diameter, where x is the coordinate along the axis of the duct.

To obtain the mean friction factor in a duct, for a perfect gas under adiabatic flow conditions, it is sufficient to know the values of Mach number at the limiting sections of the length L of the duct where the friction losses have to be evaluated. The following equation [12], is then used:

$$\bar{f} \frac{L_{max}}{D} = \frac{1 - M^2}{kM^2} + \frac{k + 1}{2k} \ln \frac{(k + 1)M^2}{2(1 + \frac{k-1}{2} M^2)} \tag{3.7}$$

where L_{max} is the maximum possible length of the duct with a limiting Mach number value equals to unity, and $\bar{f}$ is the mean friction factor with respect to length, defined by

$$\bar{f} = \frac{1}{L_{max}} \int_0^{L_{max}} f \, dx .$$

The application of equation (3.7) on sections 1' and 2 yields

$$\bar{f} \frac{L}{D} = (\bar{f} \frac{L_{max}}{D})_{M_1'} - (\bar{f} \frac{L_{max}}{D})_{M_2} \tag{3.8}$$

Using equation (3.8), we obtain the value of $\bar{f}\,\frac{L}{D}$ between the section 1' where $M = M_1'$ and the section 2 where $M = M_2$.

At section 1' the Mach number M_1' is calculated using the relation $M_1' = M_1 \frac{A_1}{A_2}$. This equation is obtained from the continuity equation between sections 1 and 1' where the flow is assumed to be incompressible and isothermal.

Fourth Assumption:

Using a parallel analysis to that for adiabatic flow, the friction factor in a duct, for a perfect gas under isothermal flow conditions, can be obtained using the equation

$$f\,\frac{L_{max}}{D} = \frac{1 - kM^2}{kM^2} + \ln kM^2 \tag{3.9}$$

where L_{max} is the maximum possible length of duct with a limiting Mach number equal to $1/\sqrt{k}$ [12]. Hence:

$$f\,\frac{L}{D} = \left(\frac{f\,L_{max}}{D}\right)_{M_1'} - \left(\frac{f\,L_{max}}{D}\right)_{M_2} \tag{3.10}$$

From equation (3.10) we can calculate the value of $f\,\frac{L}{D}$ between the section 1' where $M = M_1'$ and the section 2 where $M = M_2$ under isothermal flow conditions.

$M_1' = M_1 \frac{A_1}{A_2}$ as mentioned for adiabatic flow.

The values of the entrance correction factor, K, obtained for incompressible and compressible, isothermal flow processes are listed in Table 5. The values obtained for the adiabatic flow process are listed in Table 6. These values are defined as follows:

- K (laminar) is the value of K calculated using the incompressible, laminar flow friction factor ($f = \frac{64}{Re}$) under the exit conditions obtained for adiabatic flow.
- K (turbulent) is the value of K calculated using the incompressible, turbulent friction factor ($f = 0.316/Re^{\frac{1}{4}}$) under the exit conditions obtained for adiabatic flow.
- K (Fanno) is the value of K calculated using Fanno equation to evaluate the friction factor (f) for adiabatic frictional flow.

The variation of the value of K vs. Reynold's number is represented on Figure 10.

The values of K, in the laminar flow region are obtained from Table 5 for incompressible, laminar flow up to a Reynold's number of about 3,000 which corresponds to a Mach number of about 0.25. The values of K for the transition and turbulent regions are obtained from Table 6 for adiabatic flow process (K-Fanno).

A similar pattern of the curve obtained in the present work (Fig. 9) was obtained by Olson [14] for rounded edge entrances and by Lakshmana and Nagar [22].

The pressure drop evaluated values are given in Tables 7 and 8. The value of the entrance correction factor (K) used in the calculation of the pressure drop is K = 1.39 which is the value given by Olson [16] for fully developed flow. The values of Δp indicated in Table 8 as Δp (laminar), Δp (turbulent) and Δp (Fanno) represent the calculated values using different friction factors (f) in the same way as for the entrance correction factor.

Figure 11 represents the theoretical pressure drop evaluated using incompressible, laminar flow equations up to Reynold's number of about 3000 (Mach number of about 0.25) and adiabatic flow equations for higher values of Reynold's number, compared to the measured values of the pressure drop.

It is shown from Figure 11 that the evaluated pressure drop is higher than the measured pressure drop for all measured values up to 12 psi.

The discrepancy observed would be greater if the entrance correction factor used was higher than 1.39.

CHAPTER IV

DISCUSSION OF RESULTS

CHAPTER IV

DISCUSSION OF RESULTS

4.1 Summary of Results

1- Comparison of the values of C_q calculated from Equations (2.4), (2.6) and (2.10) shows that all values are the same up to a pressure differential of 2.9 psi. The corresponding limiting values are $\lambda \approx 7x10^3$, Re $\approx 6.5x10^3$ and $M \approx 0.5$. Below these limiting values, the flow can be treated as incompressible. Any volume flow rate can be conveniently calculated from Equation (2.4), using the value of C_q obtained from Figure 7 at the corresponding value of λ which is given by Equation (2.18). No prior knowledge of the nozzle exit conditions is required.

2- At pressure differential higher than 2.9 psi, the adiabatic and isothermal processes give identical values of C_q at corresponding values of pressure differential (Tables 3 and 4). The values of λ and Re change for the two processes because they are based on exit conditions which differ for adiabatic and isothermal flow. Nevertheless, the plots of C_q vs. Re and λ give values of C_q at corresponding values of λ and Re that agree within approximately 2%. The smallest deviation occurs in the plot of C_q vs. λ, (Fig. 7). The adiabatic exit flow for a given pressure differential is conveniently obtained by first finding the isentropic exit Mach number and temperature which yields the isentropic exit velocity. The next step is to calculate the exit flow number (Equation (2.29)) and to obtain the value of C_q' from Figure 7. The actual exit velocity is the product of C_q' and the isentropic exit velocity.

3- Pressure drop calculations are complicated by the fact that the flow is partially developed, is laminar, and incompressible for low pressure differentials, is turbulent and compressible for high pressure differentials and it falls in the transitional compressible range for intermediate pressure differentials. Most available theoretical and experimental data for orifices, tubes and nozzles are restricted to laminar or turbulent incompressible flow. The comparison between calculated and measured pressure drops shows maximum deviation in the middle range (Fig. 11). The selection of the entrance loss coefficient K is another complicating factor in the computation of the pressure drop.

The experimental results obtained for the entrance correction factor in the present study agrees, in the laminar flow region, (Reynold's number lower than 3000) with the theoretical values obtained by Chen [15]. The form of the obtained curve of the entrance correction factor variation (Fig. 10) is similar to those given by Olson [14] and Lakshmana [22].

The theoretically evaluated pressure drops are lower than the experimentally measured values. Figure 9 shows that the discrepancy of the theoretical and experimental curves can be attributed to the use of fully developed friction factors and entrance loss coefficients.

4.2 Recommendation for Further Research

More accurate prediction of the flow coefficient will have to take into account the velocity profile development, and the pressure gradient variation at the entrance of the nozzle.

The temperature variation at the exit of the jet nozzle will also have to be determined experimentally.

4.3 Conclusion

Although there are various aspects to be investigated, the present work should still constitute a useful contribution to the optimization of the sensor design as far as the exit velocity of the power jet is concerned.

REFERENCES

1. Tanney, J.W., "Apparatus for Measuring the Velocity of a Fluid", U.K. Patent No. 1, 262, 442, February 1972.

2. Hayes, W.F., Tanney, J.W. and Templin, R.J., "The Co-Flowing Jet Velocity Sensor", Paper J 1, Fifth Cranfield Conference, University of Uppsala, June 13 - 16, 1972.

3. Kuchemann, D. and Weber, J., "Aerodynamics of Propulsion", McGraw-Hill, 1953.

4- Squire, H.B. and Trouncer, J., "Round Jets in General Stream", A.R.C. R & M No. 1974, January 1944.

5- Wang, R.L. and duPlessis, M.P., "An Explicit Numerical Method for the Solution of Jet Flows", J. Fluids Engineering Transactions of the ASME 95, pp. 38-46, 1973.

6- duPlessis, M.P., Wang, R.L. and Tsang, S., "Development of a Submerged Round Laminar Jet from an Initially Parabolic Profile", J. Dynamic Systems, Measurement, and Control. Transactions of the ASME, 95, pp. 148-154, 1973.

7- duPlessis, M.P., Wang, R.L. and Kahawita, R., "Investigation of the Near Region of a Square Jet", J. Fluids Engineering, ASME (Accepted for publication).

8- duPlessis, M.P., Hayes, W.F. and Wang, R.L., "Analytical Investigation of the Characteristics of the Co-Flowing Velocity Sensor", CSME Paper No. 73 - CSME - 70, EIC Accession No. 1528.

9- Pantatkar, S.V. and Spalding, D.B., "Heat and Mass Transfer in Boundary Layer", Intertext Books, London, 1970.

10- McCloy, O. and Martin, H.R., "The Control of Fluid Power", Longman, 1973.

11- Lichtarowicz, A., Duggins, R.K. and Markland, E., "Discharge Coefficients for Incompressible Non Cavitating Flow Through Long Orifices", J. Mech. Engng. SCI, London (Jan., 1965), Vol. 7, No. 2.

12- Shapiro, Asher H., "The Dynamics and Thermodynamics of Compressible Flow", Vol. 1, New York, Ronald Press Co., 1953.

13- Streeter, Victor L., "Fluid Mechanics", McGraw-Hill Inc., 1975.

14- Olson, R.M. and Sparrow, E.M., "Measurements of Turbulent Flow Development in Tubes and Annuli with Square or Rounded Entrances", A.I. Ch. E. Journal, Vol. 9, (1963), pp. 766-770.

15- Chen, R.Y., "Flow in the Entrance Region at Low Reynold's Numbers", Journal of Fluids Eng. ASME, Vol. 95, Ser. 1, No. 1, March 1973, pp. 153-158.

16- Olson, Reuben M., "Essentials of Engineering Fluid Mechanics", 21 Edition, International Textbook Company, 1966.

17- Friedmann, M., Gillis, J. and Liron, N., "Laminar Flow in a Pipe at Low and Moderate Reynold's Numbers", Applied Science Research, Vol. 19, 1968, pp. 426-438.

18- Langhaar, H.L., "Steady Flow in the Transition Length of a Straight Tube", J. App. Mech. 9, Trans. ASME 64:A, pp. 55-58.

19- Hornbeck, R.W., "Laminar Flow in the Entrance Region of a Pipe", Applied Science Research, Section A, Vol. 13, 1964, pp. 224-234.

20- Crane Company, "Flow Through Valves, Fittings and Pipes", Technical Paper No. 410.

21- Lundgren, T.S., Sparrow, E.M. and Starr, J.B., "Pressure Drop Due to the Entrance Region in Ducts of Arbitrary Cross-Sections", Trans. AM. Soc. Mech. Engrs., Journal of Basic Eng., Vol. 86, Series D, No. 3 (1964), pp. 620-626.

22- Lakshmana, Rao., Nagar, S., "Orifice Losses for Laminar Approach Flow", ASCE, Journal of Hydraulic Division, Vol. 98, Nov. 1972, Paper No. 9370, pp. 2015-2034.

FIGURES

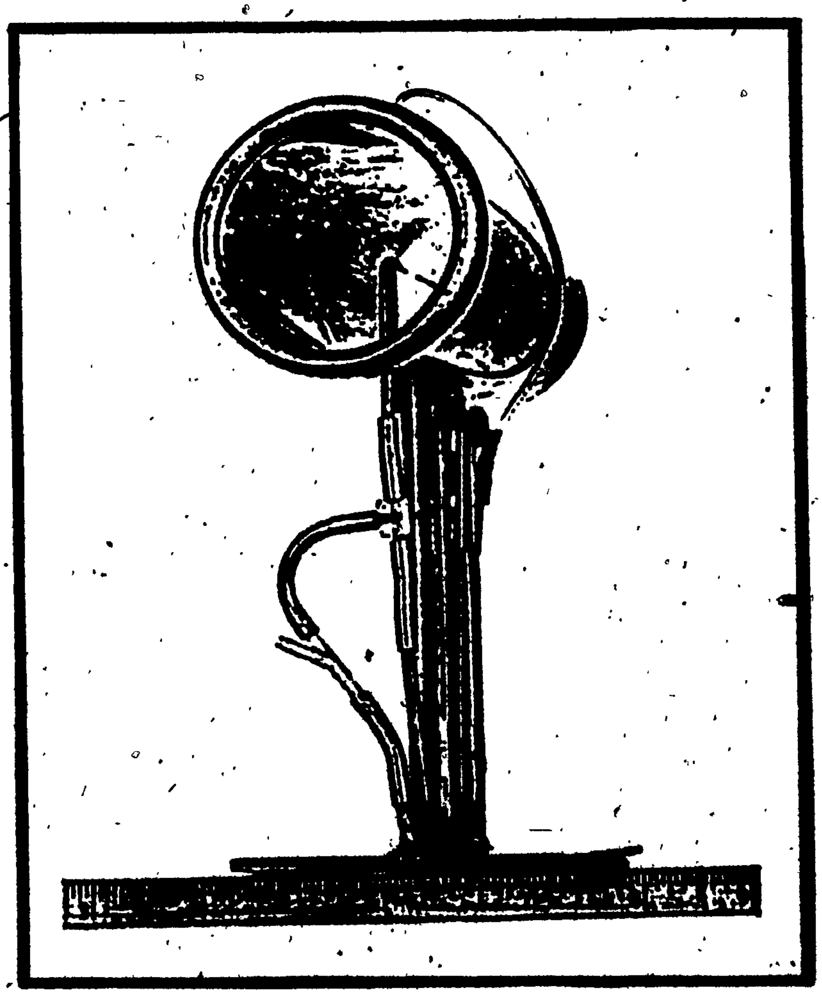

Fig. 1 Duct Mounted Co-Flowing Velocity Sensor

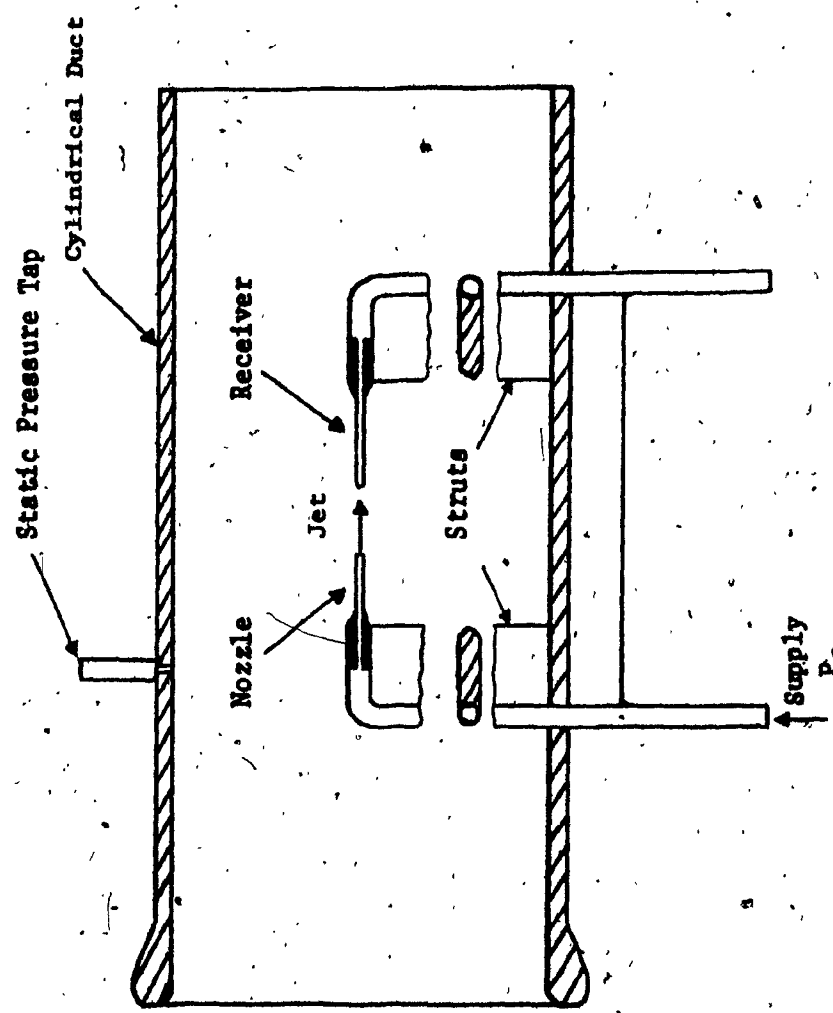

Fig. 2 Duct Flow Sensor

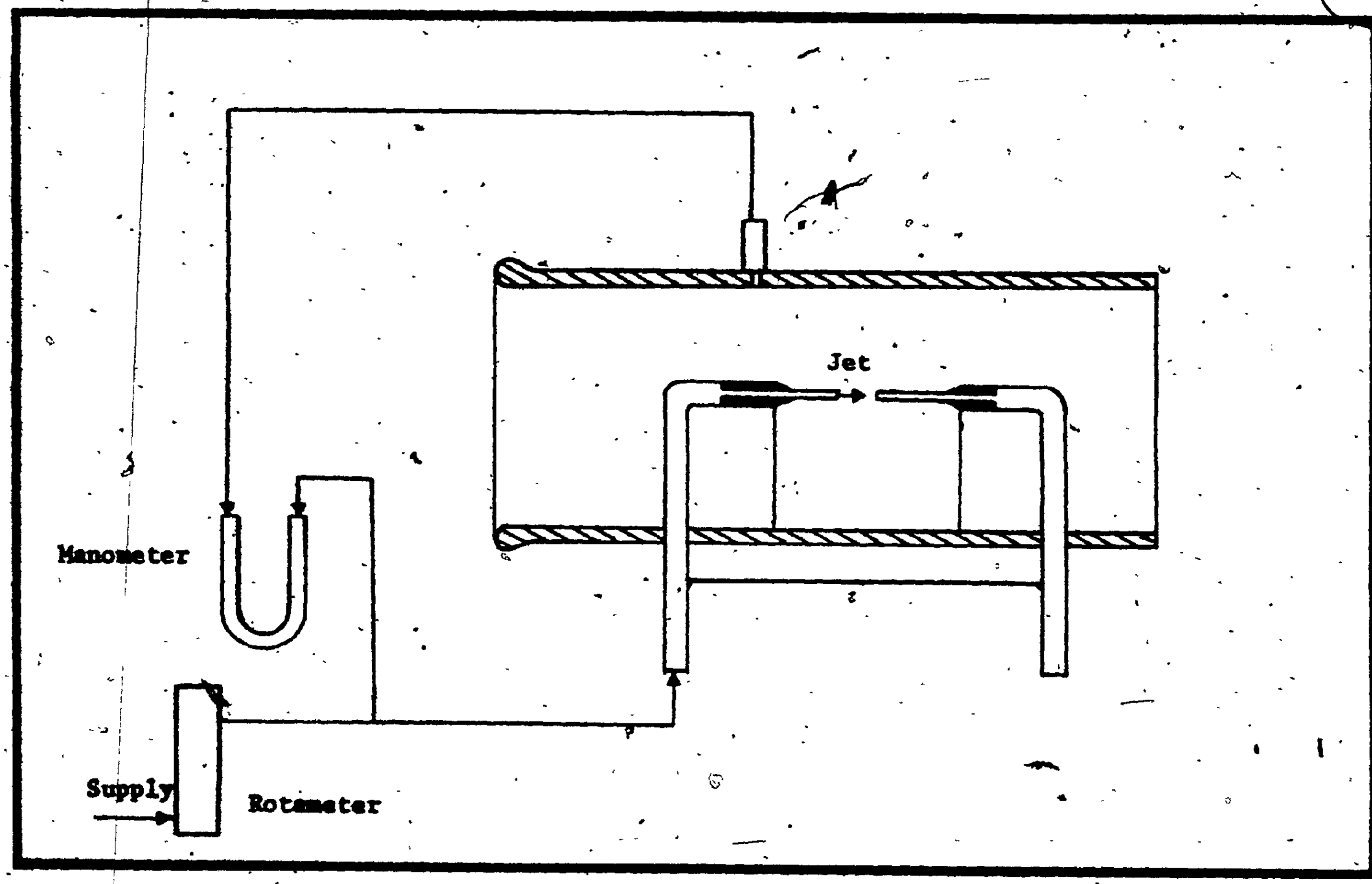

Fig. 3 Schematic Diagramm

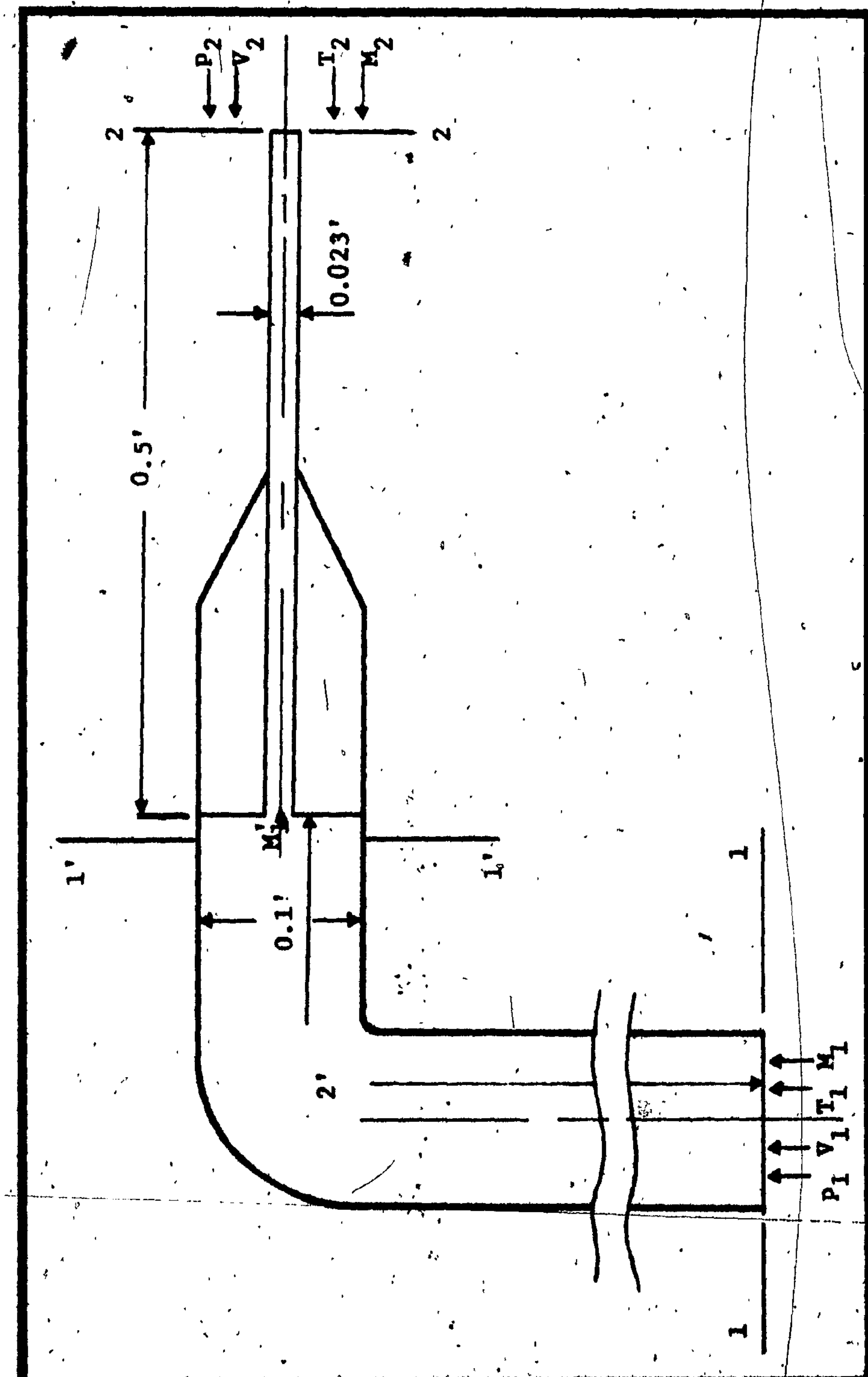

Fig. 4 Duct Dimensions.

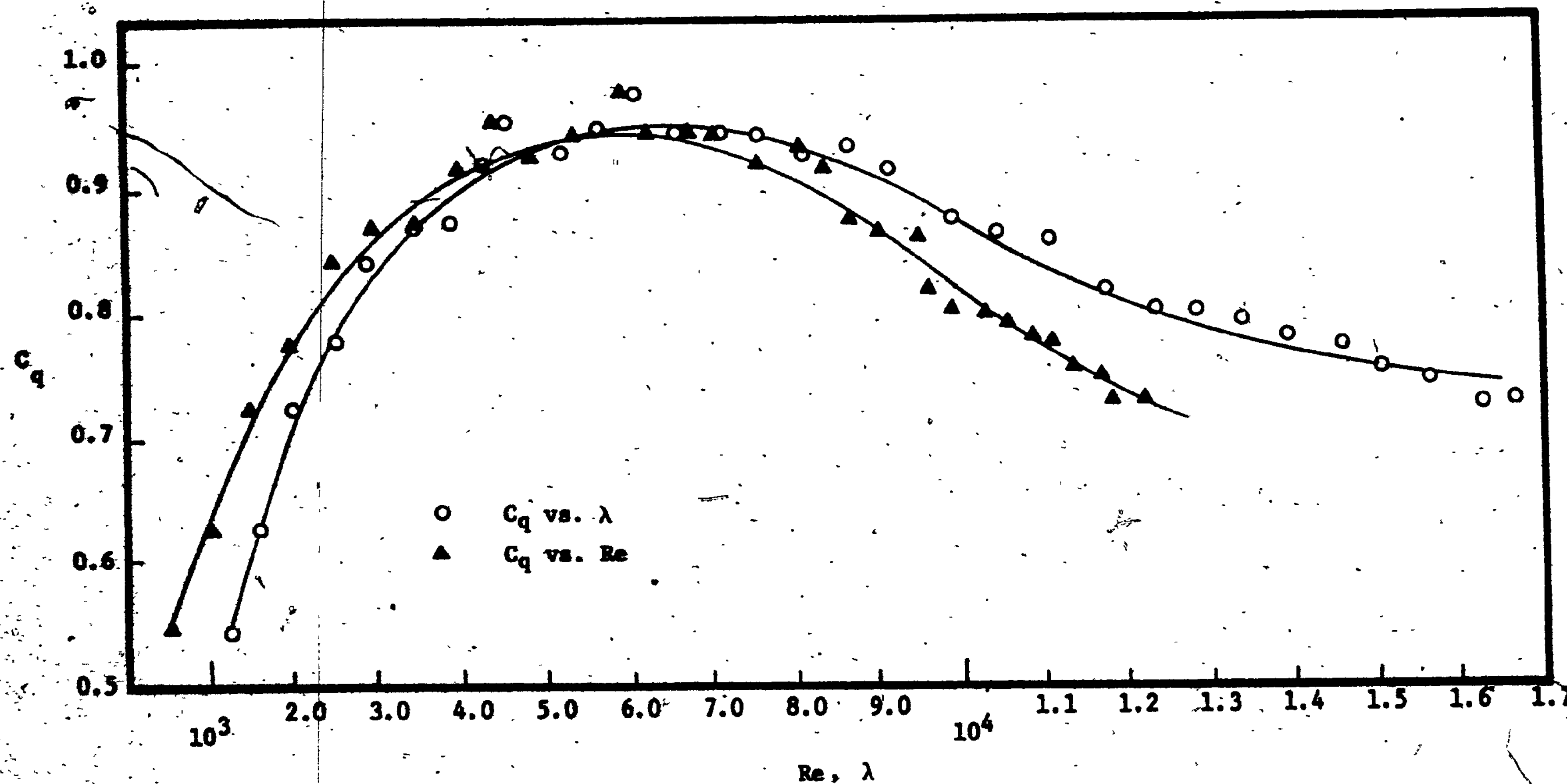

Fig. 5 Flow Coefficient Variation as a Function of Reynold's Number Compared to Flow Coefficient Variation as a Function of Flow Number for Incompressible Flow.

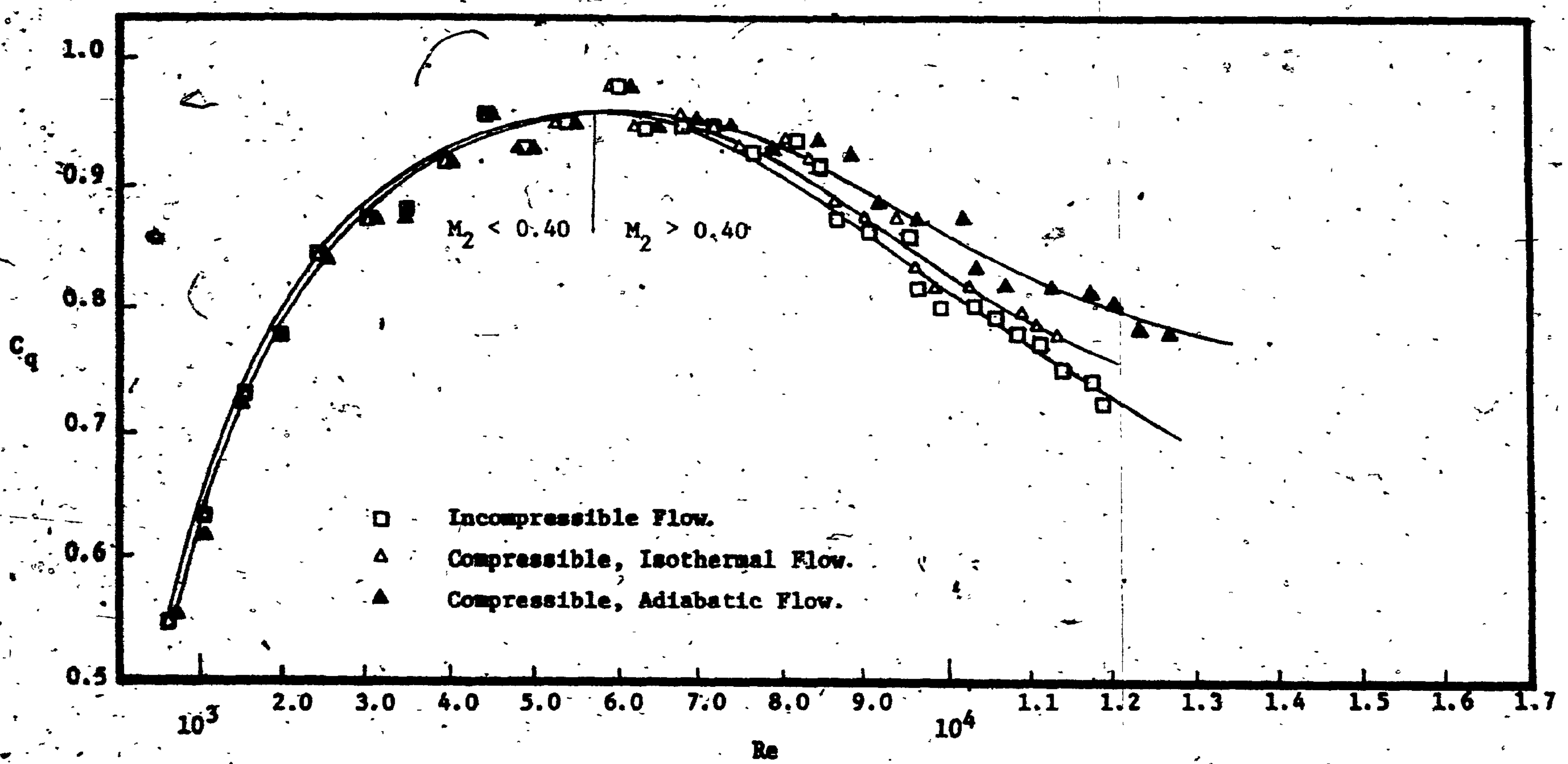

Fig. 6 Flow Coefficient Variation for Compressible Flow Compared to Flow Coefficient Variation for Incompressible Flow.

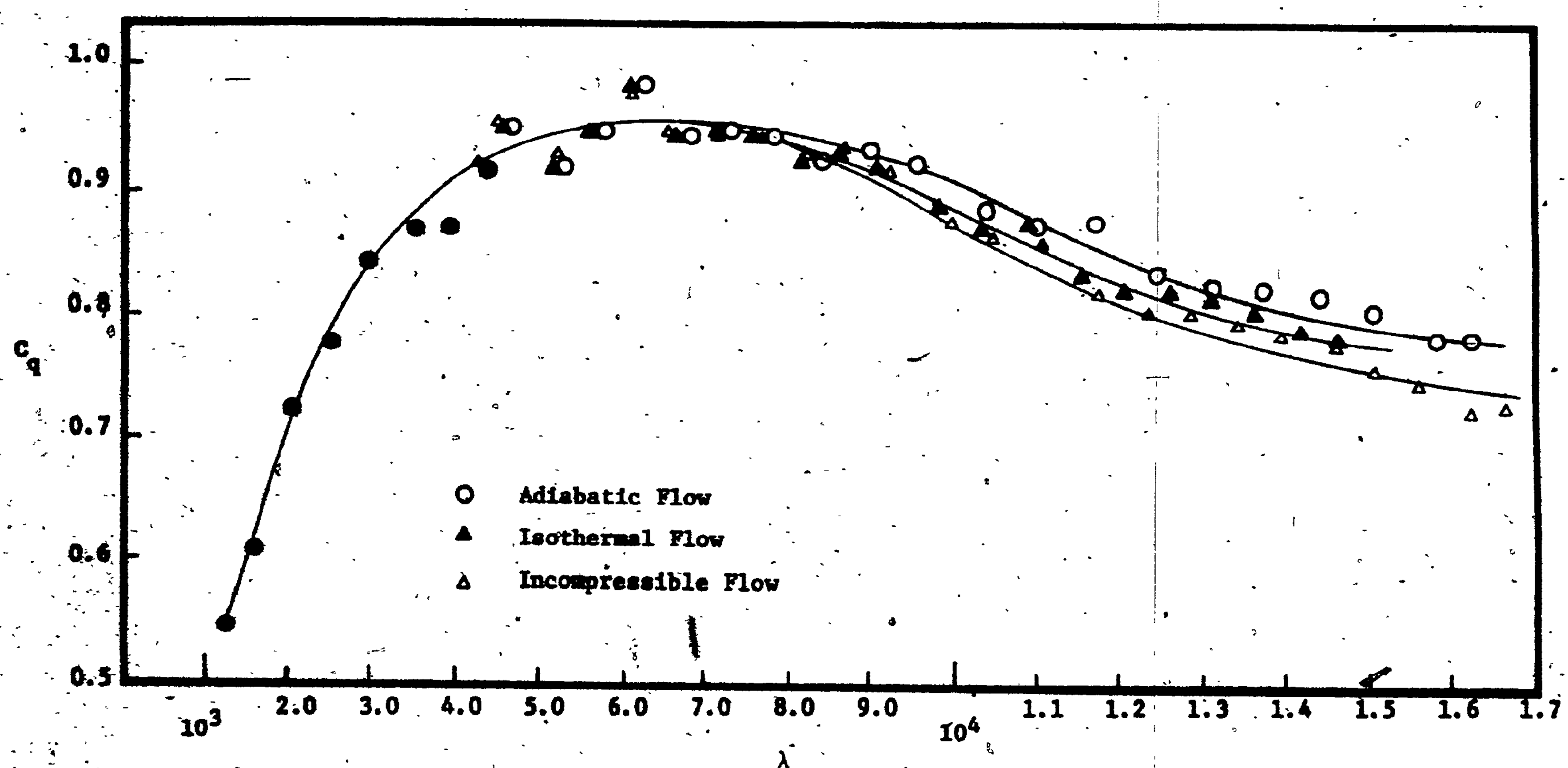

Fig. 7 Comparison Between Flow Coefficient Variation as a Function of Flow Number for Isothermal and Adiabatic Flow.

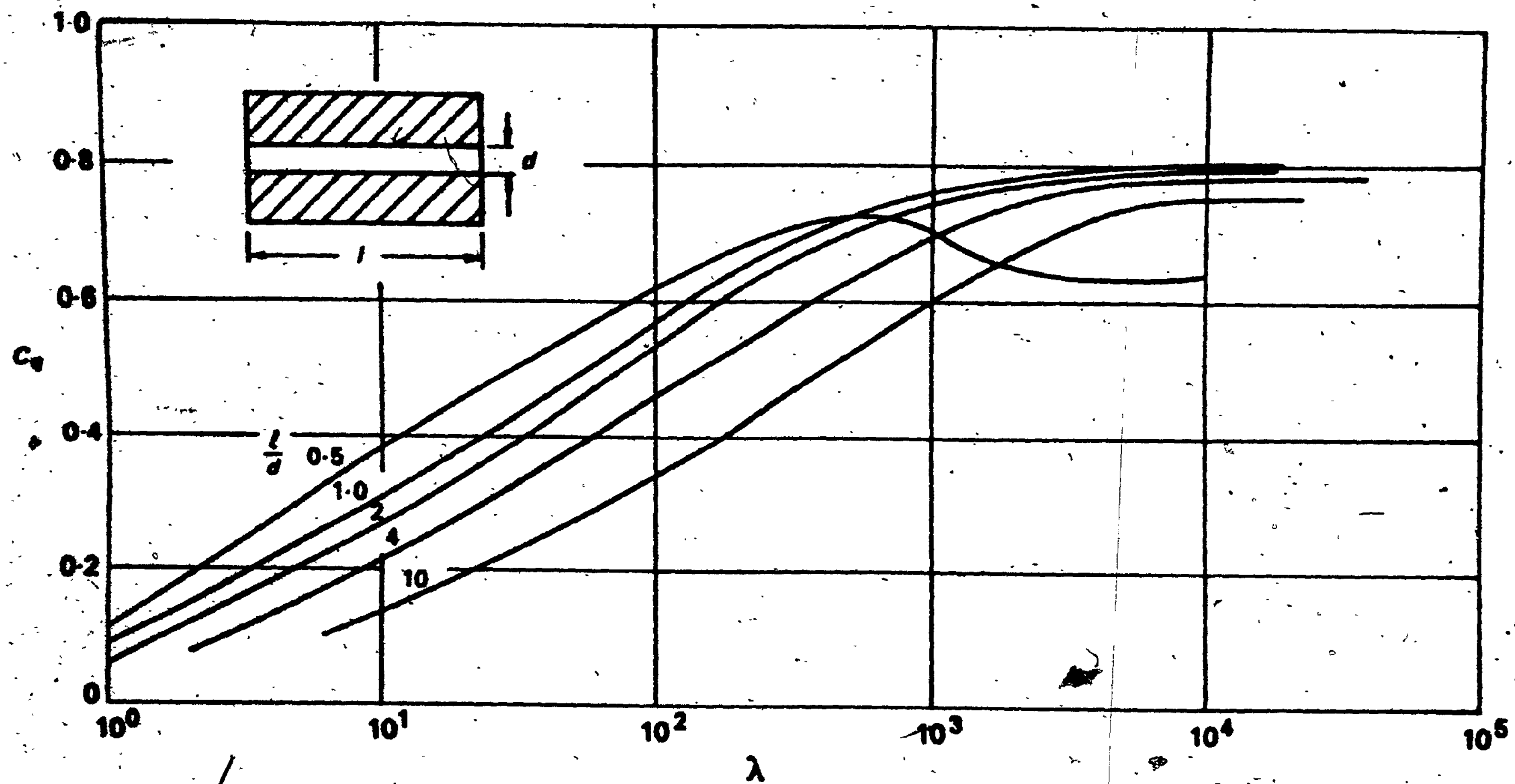

Fig. 8 Flow Coefficient of Tube Orifices after Lichtarowicz et al. [11].

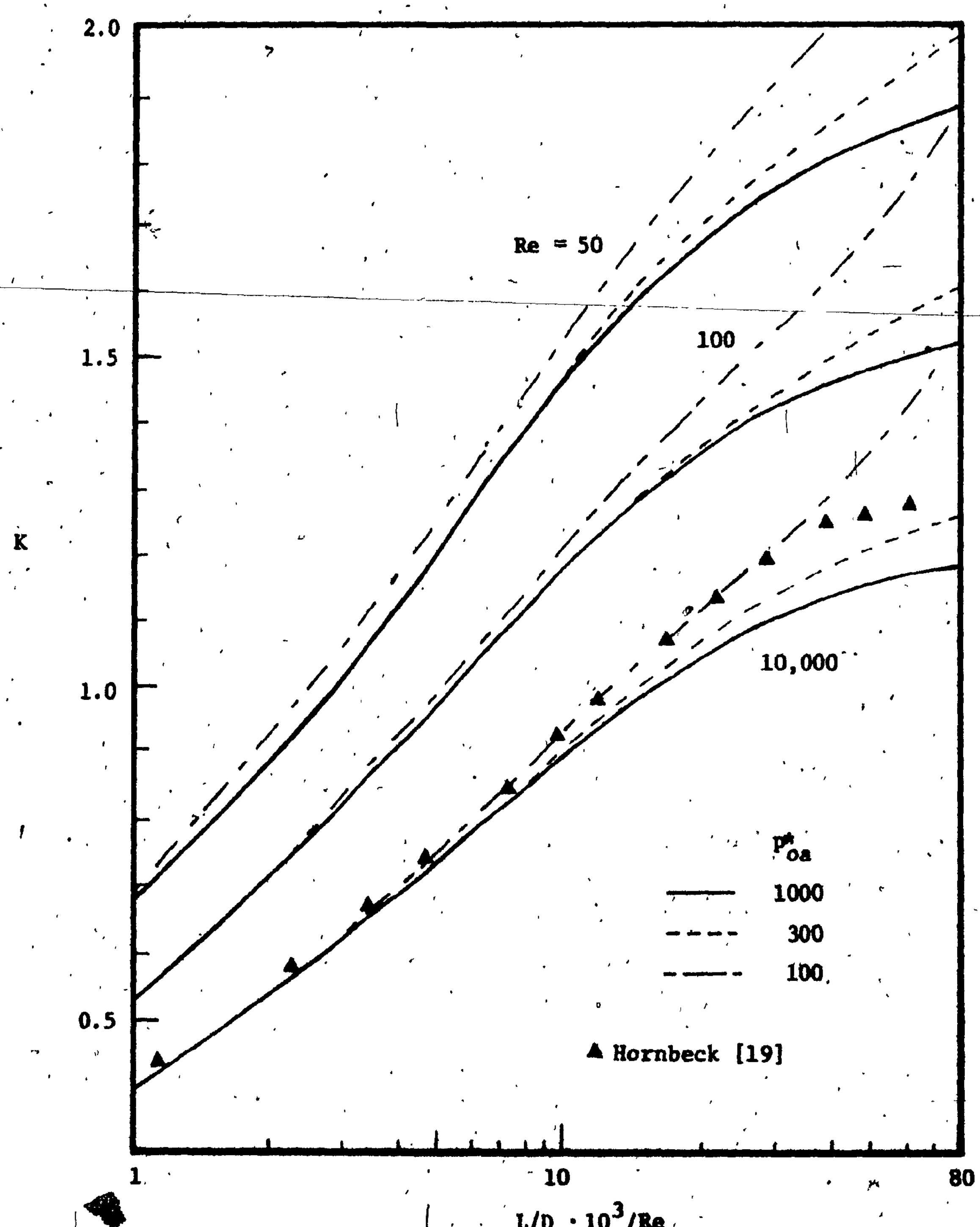

Fig. 9 Entrance Correction Factor at High Reynold's Numbers and Various p_{oa} in a Tube after CHEN R. Y. [15].

$^*p_{oa} = 2/(kM_1^2)$

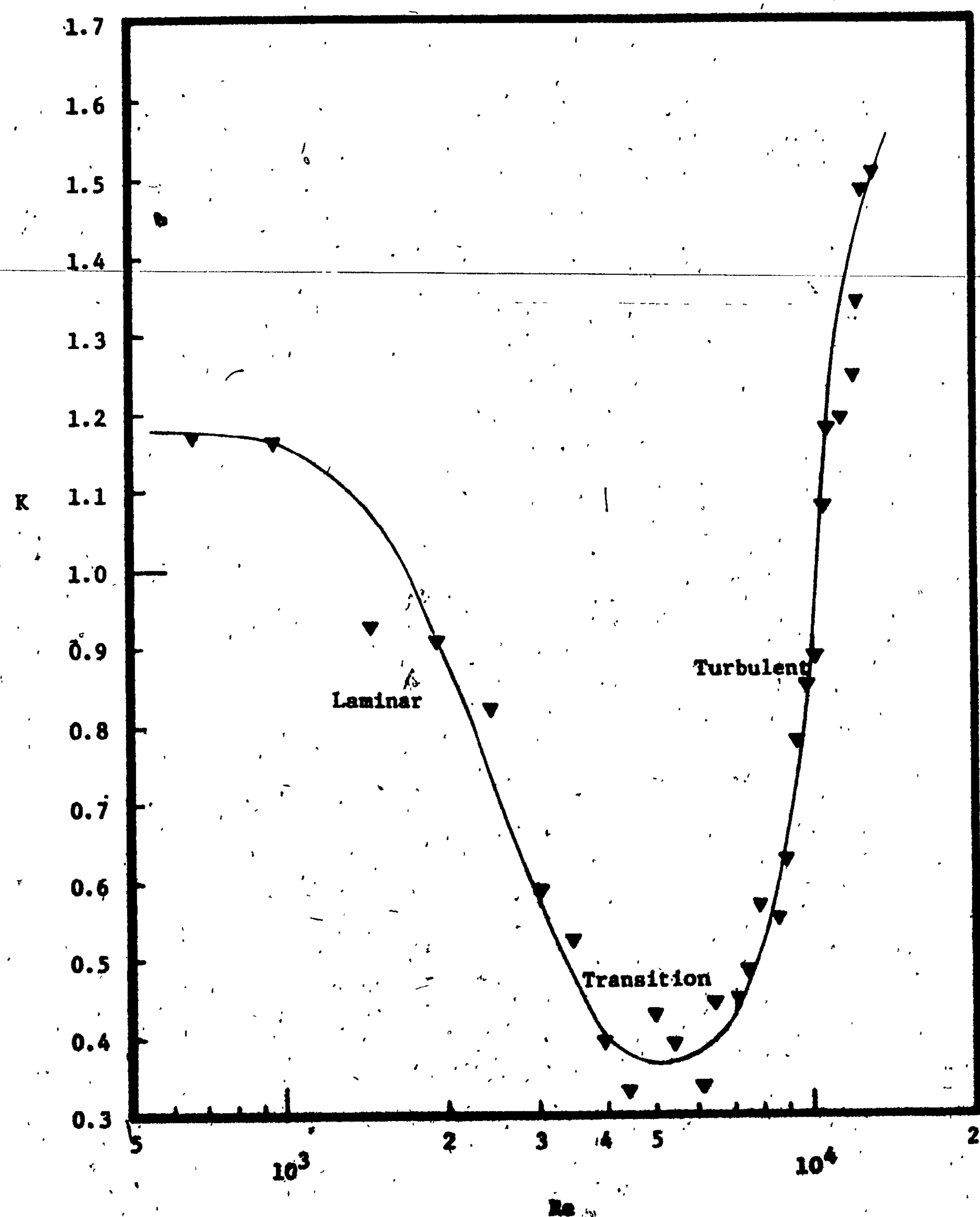

Fig. 10 Variation of the Entrance Factor as a Function of Reynold's number.

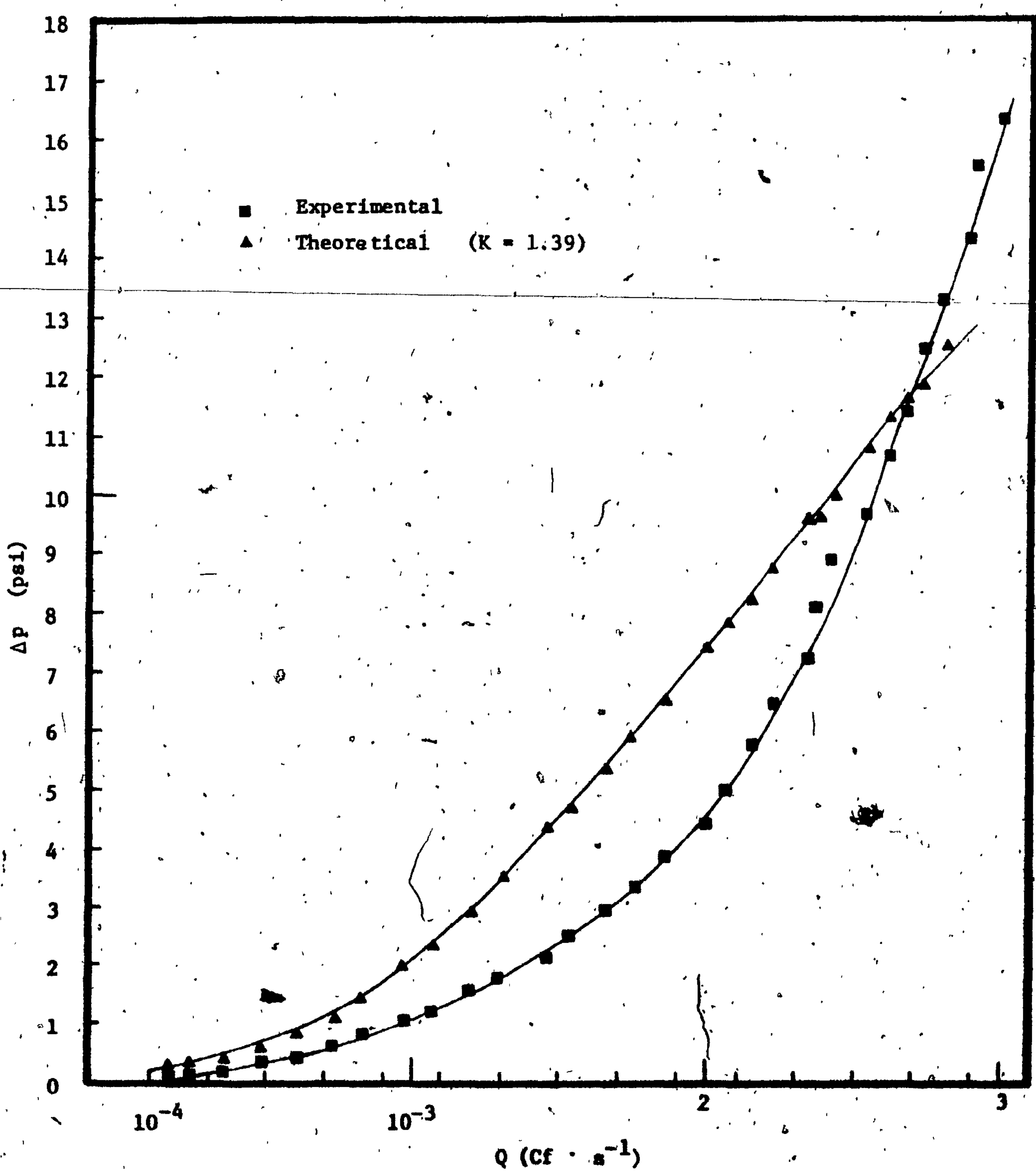

Fig. 11 **Comparison Between Experimental and Theoretical Pressure Drop Values.**

APPENDIX

COMPUTER PROGRAM TO DETERMINE THE FLOW COEFFICIENT VS. FLOW NUMBER

... FOR INCOMPRESSIBLE FLOW

```
      WRITE(6,5)
5     FORMAT('          FLOW   COEFFICIENT,INCOMPRESSIBLE')
10    READ (5,1) HW,Q,C
1     FORMAT(3F10.5)
      D1=0.1/12
      D2=0.023/12
      A1=(3.14*D1**2)/4
      A2=(3.14*D2**2)/4
      VISC=3.81/0.233
      IF(HW)4,4,2
2     G=32.2
      Q=Q/(((12.0*2.54)**3)*60*C)
      H=(HW*62.4)/(0.075*12)
      CD=Q/(A2*SQRT(2*G*H))
      RE=Q*D2/(A2*VISC)
      RE=RE*100000.0
      P=HW*0.036
      CA=1128.5
      XM=Q/(A2*CA)
      PO=P+14.7
      GAM=14.7/PO
      RE1=RE/CD
      WRITE(6,3)P,Q,CD,RE,RE1,GAM,XM
3     FORMAT(7(F11.5,2X))
      GO TO 10
4     STOP
      END
```

... FOR ADIABATIC FLOW

```
      DIMENSION  QC (29),  RE1 (29),  VISC (29),  RE (29)
      DIMENSION P(29),X(29),Y(29),V(29),Q(29),T(29)
      DIMENSION RAT(29),CAP(29),CD(29),C(29),TEX(29)
      WRITE(3,5)
5     FORMAT('          FLOW   COEFFICIENT, ADIABATIC  ')
      TO=70+460
      D2=0.023/12
      A2=(3.14*D2**2)/4
      AT=14.7
      DO 45 I=1,28
10    READ(1,15) P(I),Y(I),CAP(I)
15    FORMAT (3(F11.5))
      IF (Y(I)-1)20,20,18
18    Y(I)=1.00
20    T(I)=TO*((AT/(P(I)+14.7))**(0.4/1.4))
      C(I)=(1.4*32.2*53.3*T(I))**0.5
      V(I)=C(I)*Y(I)
      Q(I)=V(I)*A2
      Q(I)=Q(I)*TO/T(I)
      X(I)=1.40
      RAT(I)=((P(I)+14.7)/AT)**(1/X(I))
      CD(I)=CAP(I)/Q(I)
30    TEX(I)=TO*((1/RAT(I))**(X(I)-1))
      SLP=(4-3.5)/114
      VISC(I)=(SLP*(TEX(I)-460))+3.5
      RE(I)=0.00233*CAP(I)*D2/(A2*VISC(I))
      RE(I)=RE(I)*10000000.0
      RE1(I)=RE(I)/CD(I)
      WRITE(3,40) P(I),Y(I),CD(I),T(I),RE(I),RE1(I)
40    FORMAT (6(F11.4,2X))
45    CONTINUE
      STOP
      END
```

... FOR ISOTHERMAL FLOW

```
      D1 = 0.1/12
      D2= 0.023/12
      A1= 3.14 * D1 **2 /4
      A2= 3.14 * D2 * * 2 /4
      TO = 75+460
      WRITE (6,5)
5     FORMAT ( '    FLOW  COEFFICIENT ISOTHERMAL' )
      DO  50 I=1,25
      READ (5,10)P,X1,Q
10    FORMAT (3(F11.5))
      X2 = X1 *(14.7+P)* A1/(14.7*A2)
      CO= (1.4 * 32.2 * 53.3 * TO) ** 0.5
      V2 =  X2 * CO
      Q2 =  V2*A2
      CD = Q/(V2 * A2)
      RE = 0.00237 * Q * D2 / (A2 * 3.77)
      RE = RE * 10.0 **7.0
      WRITE (6,30) P, X2,Q2,Q,CD,RE
30    FORMAT (6(2X,F11.5))
50    CONTINUE
      STOP
      END
```

COMPUTATION OF THE ENTRANCE COEFFICIENT FOR ADIABATIC FLOW

```
      D1=0.1/12
      D2=0.023/12
       TO=70+460
       L=2/12
       WRITE (6,5)
5     FORMAT ( 'ENTRANCE COEFFICIENT ADIABATIC')
      DO 50 I=1,28
       READ (5,10)XO,X2,P,T,CD
10     FORMAT (5(F11.5))
       CO = (1.4*32.2*53.3*TO)**0.5
       VO = XO*CO
       C2 =(1.4*32.2*53.3*T)**0.5
       V2T =C2* X2
       V2= V2T*CD
      DEN1=0.00233*(14.7+P)/14.7
      REO=DEN1*VO*D1/3.81
       REO =REO* 10.0**7.0
20     FO1 = 64/ REO
      DEN2=0.00233*TO/T
        SLP =(4-3.5)/114
       VISC2 =(SLP*(T-460))+3.5
       RE2 =DEN2*V2 *D2/VISC2
      RE2=RE2*10.0**7.0
30    FO2=64/RE2
35    FO21=0.316/(RE2**0.25)
      X1=XO*D1**2/(D2**2)
       DMAX1 = (1-X1**2)/ (1.4*X1**2)
      DMAX1=DMAX1+(0.857*ALOG((1.2*X1**2)/((0.2*X1**2)+1)))
       DMAX2=(1-X2**2)/(1.4*X2**2)
      DMAX2=DMAX2+(0.857*ALOG((1.2*X2**2)/((0.2*X2**2)+1)))
      FO22=(DMAX1-DMAX2)/21.74
       DELP1=FO1*DEN1*VO**2*(L/D1+3)/(2*144)
      BOUT=DEN2*V2**2/(2*144)
      ETA =(P/BOUT)-(FO2 *21.74)
      ETA1=(P/BOUT)-(FO21*21.74)
      ETA2=(P/BOUT)-(FO22*21.74)
      WRITE(6,45) P,ETA,ETA1,ETA2,REO,RE2,DELP1
45     FORMAT(4(F11.3),2X,2(F9.3,2X),F9.5)
50      CONTINUE
        STOP
        END
```

COMPUTATION OF THE INLET AND EXIT MACH NUMBER FOR ISENTROPIC FLOW

```
      DIMENSION P(28),X(28),ALP(28),BET(28),DEL(28),Y(28)
      WRITE(6,5)
 5    FORMAT(' MACH NUMBER')
      D1=0.1
      D2=0.023
      GAM=(D1/D2)**2.0
      AT=14.7
      DO 80 I=1,29
 10   READ(5,11) P(I),X(I)
 11   FORMAT (F11.5,F10.5)
      E=AT+P(I)
      ALP(I)=(AT/E)**0.2857
 15   DO 60 J=1,30
      X(I)=X(I)+0.00005
 18   Y(I)=((1+0.20*X(I)**2)/(0.20*ALP(I))-5)**0.5
 40   BET(I)=GAM*(1+0.20*Y(I)**2)**3/Y(I)
      DEL(I)=(1+0.2*X(I)**2)**3/X(I)
 45   WRITE(6,50) P(I),X(I),Y(I),ALP(I),BET(I),DEL(I)
 50   FORMAT (6(F11.5,3X))
 60   CONTINUE
 80   CONTINUE
 85   STOP
      END
```

COMPUTATION OF THE ENTRANCE COEFFICIENT FOR ISOTHERMAL FLOW

```
      D1 = 0.1/12
      D2 = 0.023/12
      TO=70+460
      L = 2/12
      WRITE (6,5)
 5    FORMAT (' ENTRANCE COEFFICIENT,ISOTHERMAL')
      DO 50 I=1,28
      READ(5,10) XO,X2,P,CD
 10   FORMAT (4(F11.5))
      CO = (1.4*32.2*53.3*TO)**0.5
      VO = CO * XO
      C2 = CO
      V2 = X2 * C2*CD
      DEN1=0.00233*(P+14.7)/14.7
      REO =DEN1*VO*D1/3.81
      REO = REO * 10.0 ** 7.0
      FO1 = 64/REO
      DELP1=FO1*DEN1*VO**2*(L/D1+3)/(2*144)
      RE2 = 0.00233*V2*D2/3.81
      RE2 = RE2 * 10.0 ** 7.0
 30   FO2 = 64/RE2
      FO21=0.316/(RE2**0.25)
 35   X1=XO*D1**2/D2**2
      GAM=1/(1.4*X1**2)
      DMX1=GAM-1
      DMX1=DMX1-ALOG(GAM)
      GAM1=1/(1.4*X2**2)
      DMX2=GAM1-1
      DMX2=DMX2-ALOG(GAM1)
      FO22=(DMX1-DMX2)/21.74
      DEN2=0.00233
      ROUT=DEN2*V2**2/(2*144)
      ETA =(P/ROUT)-(FO2 *21.74)
      ETA1=(P/ROUT)-(FO21*21.74)
      ETA2=(P/ROUT)-(FO22*21.74)
      WRITE(6,45) P,ETA,ETA1,ETA2,REO,RE2,DELP1
 45   FORMAT(4(F11.3),2X,2(F9.3,2X),F9.5)
 50   CONTINUE
      STOP
      END
```

COMPUTER PROGRAM TO EVALUATE THE PRESSURE DROP ACROSS THE NOZZLE FOR ISOTHERMAL FLOW

```
      D1 = 0.1/12
      D2 = 0.023/12
      T0=70+460
      L = 2/12
      WRITE (6,5)
    5 FORMAT( 'PRESSURE DROP EVALUATION ISOTHERMAL')
      DO 50 I=1,28
      READ(5,10) X0,X2,P,CD
   10 FORMAT (4(F11.5))
      C0 = (1.4*32.2*53.3*T0)**0.5
      V0 = C0 * X0
      C2 = C0
      V2 = X2 * C2*CD
       DEN1=0.00233*(P+14.7)/14.7
       RE0 =DEN1*V0*D1/3.81
      RE0 = RE0 * 10.0 ** 7.0
      F01 = 64/RE0
      DELP1=F01*DEN1*V0**2*(L/D1+3)/(2*144)
      RE2 = 0.00233*V2*D2/3.81
      RE2 = RE2 * 10.0 ** 7.0
   30 F02 = 64/RE2
      F021=0.316/(RE2**0.25)
   35 X1=X0*D1**2/D2**2
      GAM=1/(1.4*X1**2)
      DMX1=GAM-1
      DMX1=DMX1-ALOG(GAM)
      GAM1=1/(1.4*X2**2)
      DMX2=GAM1-1
       DMX2=DMX2-ALOG(GAM1)
      F022=(DMX1-DMX2)/21.74
      DEN2=0.00233
      BOUT=DEN2*V2**2/(2*144)
      ETA =BOUT*((F02 *21.74)+1.39)
      ETA1=BOUT*((F021*21.74)+1.39)
      ETA2=BOUT*((F022*21.74)+1.39)
      RATIO=P/ETA
      RATIO1=P/ETA1
      RATIO2=P/ETA2
      WRITE(6,45) P,ETA,ETA1,ETA2,RATIO,RATIO1,RATIO2,RE2
   45 FORMAT(4(F9.3),2X,3(F8.3),2X,F9.3)
   50 CONTINUE
      STOP
      END
```

... FOR ADIABATIC FLOW

```
      D1=0.1/12
      D2=0.023/12
       T0=70+460
       L=2/12
       WRITE (6,5)
5     FORMAT( 'PRESSURE DROP EVALUATION ADIABATIC')
      DO 50 I=1,28
       READ (5,10)X0,X2,P,T,CD
10     FORMAT (5(F11.5))
       C0 = (1.4*32.2*53.3*T0)**0.5
       V0 = X0*C0
       C2 =(1.4*32.2*53.3*T)**0.5
       V2T =C2* X2
       V2= V2T*CD
      DEN1=0.00233*(14.7+P)/14.7
      RE0=DEN1*V0*D1/3.81
       REO =RE0* 10.0**7.0
20     F01 = 64/ REO
      DEN2=0.00233*T0/T
        SLP =(4-3.5)/114
       VISC2 =(SLP*(T-460))+3.5
       RE2 =DEN2*V2 *D2/VISC2
      RE2=RE2*10.0**7.0
30    F02=64/RE2
35    F021=0.316/(RE2**0.25)
      X1=X0*D1**2/(D2**2)
       DMAX1 = (1-X1**2)/ (1.4*X1**2)
      DMAX1=DMAX1+(0.857*ALOG((1.2*X1**2)/((0.2*X1**2)+1)))
       DMAX2=(1-X2**2)/(1.4*X2**2)
      DMAX2=DMAX2+(0.857*ALOG((1.2*X2**2)/((0.2*X2**2)+1)))
      F022=(DMAX1-DMAX2)/21.74
       DELP1=F01*DEN1*V0**2*(L/D1+3)/(2*144)
      BOUT=DEN2*V2**2/(2*144)
      ETA =BOUT*((F02 *21.74)+1.39)
      ETA1=BOUT*((F021*21.74)+1.39)
      ETA2=BOUT*((F022*21.74)+1.39)
       RATIO=ETA/P
      RATIO1=ETA1/P
      RATIO2=ETA2/P
      WRITE(6,45) P,ETA,ETA1,ETA2,RATIO,RATIO1,RATIO2,RE2
45    FORMAT(4(F9.3),2X,3(F8.3),2X,F9.3)
50        CONTINUE
          STOP
          END
```

Table no 1

MACH NUMBERS FOR ISENTROPIC FLOW

Pressure differential Psi	Mach number at the inlet of the duct	Mach number at the nozzle exit
0.828	0.00472	0.08972
0.137	0.00605	0.11526
0.227	0.00774	0.14825
0.353	0.00957	0.18462
0.475	0.01101	0.21395
0.684	0.01317	0.25605
0.882	0.01461	0.29008
1.076	0.01591	0.31974
1.224	0.01681	0.34038
1.613	0.01882	0.38898
1.861	0.01990	0.41670
2.164	0.02106	0.44777
2.596	0.02247	0.48815
2.984	0.02354	0.52126
3.377	0.02446	0.55220
3.917	0.02555	0.59142
4.406	0.02638	0.62422
4.921	0.02711	0.65634
5.778	0.02811	0.70539
6.415	0.02866	0.73888

Table no 1 (continued)

MACH NUMBERS FOR ISENTROPIC FLOW

Pressure differential Psi	Mach number at the inlet of the duct	Mach number at the nozzle exit
7.196	0.02922	0.77707
8.078	0.02970	0.81698
8.910	0.03003	0.85197
9.695	0.03029	0.88295
10.577	0.03044	0.91573
11.408	0.03055	0.94489
12.485	0.03062	0.98042
13.316	0.03064	1.00000

TABLE 2

FLOW COEFFICIENT FOR INCOMPRESSIBLE FLOW

FLOW COEFFICIENT INCOMPRESSIBLE

ΔP_s(psi)	Q	C_q	Re_2	λ	$\frac{p}{p_o}$	M_2
0.08250	0.00016	0.54379	645.92603	1187.83081	0.99440	0.04883
0.13680	0.00023	0.62488	954.06689	1526.80347	0.99378	0.07213
0.22680	0.00035	0.72507	1425.41357	1965.90088	0.98481	0.10776
0.35280	0.00047	0.77436	1898.66699	2451.90845	0.97656	0.14354
0.47520	0.00059	0.84153	2394.69165	2845.62891	0.96869	0.18104
0.68400	0.00073	0.86724	2960.79346	3414.03491	0.95554	0.22384
0.88200	0.00083	0.87118	3377.39453	3876.80884	0.94340	0.25533
1.07640	0.00097	0.91749	3929.41479	4282.73906	0.93177	0.29705
1.22400	0.00107	0.95242	4349.67578	4566.99219	0.92313	0.32883
1.61280	0.00119	0.92560	4852.34766	5242.39844	0.90113	0.36684
1.86120	0.00131	0.94710	5333.76953	5631.66016	0.88762	0.40323
2.16360	0.00146	0.97761	5936.00000	6071.95313	0.87170	0.44876
2.59560	0.00154	0.94384	6277.10156	6650.56641	0.84993	0.47455
2.98440	0.00166	0.94627	6748.12500	7131.28906	0.83124	0.51015
3.37680	0.00175	0.93760	7112.30469	7585.64453	0.81320	0.53769
3.91680	0.00186	0.92404	7549.09375	8169.68359	0.78961	0.57071
4.40640	0.00199	0.93238	8079.33203	8665.26953	0.76938	0.61080
4.92120	0.00206	0.91605	8388.65625	9157.46875	0.74919	0.63418
5.77800	0.00214	0.87486	8680.99609	9922.67188	0.71784	0.65628
6.41520	0.00222	0.86185	9011.07031	10455.50391	0.69518	0.68124
7.19640	0.00234	0.85882	9510.45703	11073.32031	0.67134	0.71899
8.07840	0.00236	0.81691	9584.62109	11732.62422	0.64535	0.72460
8.91000	0.00243	0.80259	9889.51172	12321.32578	0.62262	0.74765
9.69479	0.00254	0.80265	10316.53125	12853.13672	0.60259	0.77993
10.57679	0.00263	0.79504	10673.42969	13425.07813	0.58156	0.80691
11.40840	0.00268	0.78050	10882.35938	13942.37500	0.56304	0.82270
12.48479	0.00273	0.75978	11082.07422	14585.81641	0.54074	0.83780
13.31640	0.00279	0.75379	11354.96328	15063.76563	0.52469	0.85843
14.44320	0.00288	0.74612	11705.28516	15688.15234	0.50441	0.88492
15.61579	0.00291	0.72559	11936.57031	16313.07813	0.48488	0.89484
16.35120	0.00300	0.73142	12209.08594	16692.24219	0.47341	0.92300
18.06479	0.00300	0.69540	12200.83203	17545.12500	0.44865	0.92238

TABLE 3

FLOW COEFFICIENT FOR COMPRESSIBLE ISOTHERMAL FLOW

FLOW COEFFICIENT, ISOTHERMAL

Δp_s(psi)	M_2	C''_q	Re_2	λ
0.0828	0.0897	0.5479	650.3262	1186.8391
0.1368	0.1154	0.6123	934.8440	1526.8240
0.2268	0.1486	0.7239	1422.5886	1965.1743
0.3528	0.1852	0.7796	1910.3323	2450.3191
0.4752	0.2149	0.8438	2398.0781	2841.9436
0.6840	0.2586	0.8676	2967.1143	3420.0986
0.8820	0.2926	0.8718	3373.5659	3869.6309
1.0764	0.3228	0.9234	3942.6018	4269.4453
1.2240	0.3442	0.9552	4349.0547	4553.1641
1.6128	0.3948	0.9267	4836.7969	5222.0469
1.8612	0.4238	0.9498	5324.5430	5605.8008
2.1636	0.4567	0.9823	5934.2227	6040.8984
2.5956	0.4998	0.9469	6259.3867	6610.4570
2.9844	0.5353	0.9529	6747.1328	7080.9219
3.3768	0.5686	0.9458	7112.9375	7520.9219
3.9168	0.6117	0.9294	7519.3984	8090.7578
4.4064	0.6482	0.9434	8088.4297	8573.2813
4.9212	0.6840	0.9254	8372.9492	9047.9102
5.7780	0.7402	0.8883	8698.1133	9791.3320
6.4152	0.7782	0.8766	9023.2773	10293.5430
7.1964	0.8228	0.8739	9511.0195	10882.9414
8.0784	0.8700	0.8336	9592.3086	11507.2891
8.9100	0.9118	0.8190	9876.8281	12059.9258
9.6979	0.9494	0.8221	10323.9259	12557.8320
10.5768	0.9894	0.8168	10689.7383	13087.6055
11.4084	1.0257	0.8029	10892.9648	13567.0313
12.4848	1.0704	0.7837	11096.1214	14158.7383
13.3164	1.1039	0.7766	11340.0625	14601.3984

TABLE 4

FLOW COEFFICIENT FOR COMPRESSIBLE ADIABATIC FLOW

FLOW COEFFICIENT,

ΔP_s(psi)	M_2	C'_q	T_2	Re_2	λ
0.0828	0.0897	0.5476	529.1499	651.4788	1189.7986
0.1368	0.1153	0.6124	528.5991	937.0964	1530.2588
0.2268	0.1482	0.7239	527.6865	1427.5193	1972.0332
0.3528	0.1846	0.7796	526.4207	1919.7605	2462.3789
0.4752	0.2139	0.8435	525.2041	2413.3101	2860.9014
0.6840	0.2560	0.8704	523.1575	2993.0564	3438.6978
0.8820	0.2901	0.8719	521.2493	3410.6172	3911.4988
1.0764	0.3197	0.9229	519.4060	3994.4727	4328.3711
1.2240	0.3404	0.9550	518.0259	4413.3789	4621.3516
1.6128	0.3890	0.9262	514.4680	4928.8242	5321.5469
1.8612	0.4167	0.9497	512.2515	5439.9922	5727.9922
2.1636	0.4478	0.9825	509.6099	6081.7891	6190.2500
2.5956	0.4881	0.9472	505.9402	6442.9297	6802.3594
2.9844	0.5213	0.9531	502.7368	6971.4414	7314.6250
3.3768	0.5522	0.9455	499.5942	7376.9805	7802.2813
3.9168	0.5914	0.9293	495.4104	7837.6797	8433.7930
4.4064	0.6242	0.9436	491.7495	8467.9922	8974.0156
4.9212	0.6563	0.9255	488.0281	8805.3555	9514.3594
5.7780	0.7054	0.8891	482.1047	9213.3750	10362.3203
6.4152	0.7389	0.8767	477.9026	9607.0313	10958.0664
7.1964	0.7771	0.8741	472.9675	10187.9492	11654.9180
8.0784	0.8170	0.8338	467.6611	10342.6992	12403.9805
8.9100	0.8520	0.8191	462.8943	10712.8633	13079.0547
9.6979	0.8829	0.8223	458.5732	11258.5508	13692.2305
10.5768	0.9157	0.8168	453.9597	11725.3828	14355.6758
11.4084	0.9449	0.8029	449.7805	12011.6875	14960.4180
12.4848	0.9842	0.7807	444.6187	12316.4883	15776.5914
13.3164	1.0000	0.7819	440.8071	12648.7852	16177.6016

TABLE 5

ENTRANCE CORRECTION FACTOR FOR FRICTIONAL INCOMPRESSIBLE AND COMPRESSIBLE, ISOTHERMAL, CONSTANT-AREA FLOW

ENTRANCE COEFFICIENT ISOTHERMAL

Δp_s (psi)	K laminar	K turbulent	K isothermal	Re_1	Re_2	Δp(psi) (1 - 1')
0.083	1.187	1.957	2.390	272.973	650.071	0.00016
0.137	1.171	1.417	1.704	351.170	934.624	0.00021
0.227	0.925	0.784	0.915	451.990	1422.867	0.00027
0.353	0.914	0.603	0.690	563.574	1909.765	0.00033
0.475	0.823	0.421	0.444	653.647	2398.518	0.00038
0.684	0.850	0.388	0.390	786.623	2967.556	0.00045
0.882	0.903	0.414	0.358	890.015	3374.039	0.00050
1.076	0.823	0.309	0.276	981.973	3942.669	0.00055
1.224	0.779	0.253	0.214	1047.229	4348.824	0.00058
1.613	0.883	0.347	0.313	1201.073	4836.699	0.00065
1.861	0.854	0.311	0.283	1289.336	5324.266	0.00068
2.164	0.809	0.261	0.236	1389.409	5933.922	0.00072
2.596	0.903	0.352	0.351	1520.408	6259.898	0.00077
2.984	0.907	0.355	0.368	1628.614	6747.012	0.00081
3.377	0.938	0.385	0.415	1729.820	7113.332	0.00084
3.917	0.991	0.439	0.436	1860.874	7519.832	0.00088
4.406	0.972	0.419	0.496	1971.856	8088.570	0.00091
4.921	1.026	0.474	0.577	2081.021	8372.453	0.00093
5.778	1.137	0.586	0.734	2252.009	8697.125	0.00097
6.415	1.184	0.633	0.808	2367.515	9023.184	0.00099
7.196	1.205	0.655	0.862	2503.077	9510.930	0.00101
8.078	1.346	0.797	1.044	2646.679	9592.766	0.00102
8.910	1.410	0.862	1.141	2773.782	9877.578	0.00103
9.695	1.410	0.863	1.170	2890.798	10323.828	0.00104
10.577	1.442	0.896	1.228	3010.148	10689.434	0.00105
11.408	1.505	0.960	1.319	3120.418	10893.023	0.00105
12.485	1.597	1.053	1.443	3256.509	11095.898	0.00105
13.316	1.636	1.093	1.506	3358.323	11339.508	0.00105

TABLE 6

ENTRANCE CORRECTION FACTOR FOR FRICTIONAL, COMPRESSIBLE, ADIABATIC, CONSTANT-AREA FLOW

ENTRANCE COEFFICIENT, ADIABATIC

ΔP_s (psi)	K laminar	K turbulent	K Fanno	Re_1	Re_2	Δp (psi) (1-1')
0.083	1.194	1.970	2.351	272.973	651.528	0.00016
0.137	1.180	1.423	1.835	351.170	937.124	0.00021
0.227	0.937	0.794	1.068	451.390	1427.544	0.00027
0.353	0.929	0.615	0.819	563.574	1917.657	0.00033
0.475	0.840	0.436	0.578	653.647	2413.153	0.00038
0.654	0.872	0.408	0.591	786.623	2993.017	0.00045
0.882	0.930	0.439	0.534	890.015	3410.409	0.00050
1.076	0.852	0.336	0.393	981.973	3994.630	0.00055
1.224	0.809	0.281	0.331	1047.229	4413.355	0.00058
1.613	0.924	0.386	0.432	1201.073	4928.785	0.00065
1.661	0.898	0.354	0.390	1289.336	5439.824	0.00068
2.164	0.856	0.307	0.335	1389.409	6081.871	0.00072
2.596	0.962	0.412	0.446	1520.403	6443.145	0.00077
2.984	0.974	0.422	0.454	1628.614	6971.516	0.00081
3.377	1.014	0.461	0.493	1729.314	7377.004	0.00084
3.917	1.081	0.528	0.567	1860.874	7837.457	0.00088
4.406	1.068	0.517	0.556	1971.856	8467.820	0.00091
4.921	1.137	0.585	0.630	2081.021	8805.469	0.00093
5.778	1.275	0.725	0.783	2252.009	9213.082	0.00097
6.415	1.339	0.790	0.851	2367.515	9606.863	0.00099
7.196	1.377	0.830	0.894	2503.077	10197.480	0.00101
8.078	1.555	1.009	1.082	2646.679	10342.371	0.00102
8.910	1.646	1.101	1.177	2773.782	10712.969	0.00103
9.695	1.661	1.118	1.195	2890.798	11259.020	0.00104
10.577	1.716	1.175	1.248	3010.148	11725.633	0.00105
11.409	1.808	1.268	1.341	3120.418	12011.633	0.00105
12.485	1.955	1.416	1.488	3256.509	12269.215	0.00105
13.316	1.978	1.441	1.508	3358.323	12729.590	0.00105

TABLE 7

PRESSURE DROP EVALUATION FOR

FRICTIONAL, COMPRESSIBLE, ISOTHERMAL, CONSTANT-AREA FLOW

PRESSURE DROP EVALUATION, ISOTHERMAL

Δp_s(psi)	ΔP(psi) laminar	ΔP(psi) turbulent	ΔP(psi) isothermal	$\frac{\Delta P_s}{\Delta p}$ lam.	$\frac{\Delta P_s}{\Delta p}$ turb.	$\frac{\Delta P_s}{\Delta p}$ isoth.	Re_2
0.083	0.088	0.068	0.058	0.942	1.210	1.430	650.071
0.137	0.148	0.135	0.121	0.924	1.010	1.134	934.624
0.227	0.282	0.299	0.283	0.803	0.758	0.800	1422.867
0.353	0.455	0.522	0.503	0.775	0.676	0.701	1909.765
0.475	0.667	0.803	0.796	0.712	0.591	0.597	2398.518
0.684	0.964	1.204	1.203	0.710	0.568	0.569	2967.666
0.882	1.208	1.536	1.547	0.730	0.574	0.570	3374.099
1.076	1.595	2.066	2.096	0.675	0.521	0.513	3942.669
1.224	1.904	2.490	2.533	0.643	0.492	0.483	4348.824
1.613	2.311	3.050	3.089	0.698	0.529	0.522	4836.699
1.861	2.757	3.663	3.710	0.675	0.508	0.502	5324.266
2.164	3.368	4.505	4.557	0.642	0.480	0.475	5933.922
2.596	3.720	4.990	4.994	0.698	0.520	0.520	6259.898
2.984	4.279	5.758	5.723	0.697	0.518	0.521	6747.012
3.377	4.724	6.371	6.281	0.715	0.530	0.538	7113.332
3.917	5.245	7.085	6.995	0.747	0.553	0.568	7519.832
4.406	6.013	8.146	7.851	0.732	0.541	0.561	8088.570
4.321	6.424	8.702	8.279	0.766	0.566	0.594	8372.453
5.778	6.904	9.360	8.699	0.837	0.617	0.664	8697.125
6.415	7.404	10.044	9.204	0.867	0.639	0.697	9023.184
7.196	8.193	11.110	10.009	0.879	0.648	0.719	9510.930
8.078	8.313	11.294	9.951	0.971	0.715	0.812	9592.766
8.910	8.795	11.945	10.339	1.013	0.746	0.862	9877.578
9.695	9.570	13.001	11.077	1.013	0.746	0.875	10323.828
10.577	10.229	13.899	11.664	1.034	0.761	0.907	10689.434
11.408	10.605	14.411	11.906	1.076	0.792	0.958	10893.023
12.485	10.987	14.930	12.100	1.136	0.836	1.032	11095.898
13.316	11.454	15.566	12.441	1.163	0.855	1.070	11339.508

TABLE 8

PRESSURE DROP EVALUATION FOR

FRICTIONAL, COMPRESSIBLE, ADIABATIC, CONSTANT-AREA FLOW

PRESSURE DROP EVALUATION, ADIABATIC

Δp_s (psi)	Δp (psi) laminar	Δp (psi) turbulent	Δp (psi) Fanno	$\frac{\Delta p_s}{\Delta p}$ lam.	$\frac{\Delta p_s}{\Delta p}$ turb.	$\frac{\Delta p_s}{\Delta p}$ Fanno	Re_2
0.083	0.088	0.068	0.059	0.944	1.211	1.406	651.528
0.137	0.148	0.135	0.114	0.927	1.013	1.201	937.124
0.227	0.281	0.298	0.265	0.808	0.762	0.856	1427.544
0.353	0.451	0.518	0.475	0.782	0.681	0.743	1919.657
0.475	0.660	0.795	0.748	0.720	0.598	0.636	2413.153
0.684	0.949	1.187	1.093	0.721	0.576	0.626	2993.017
0.882	1.185	1.509	1.446	0.744	0.585	0.610	3410.409
1.076	1.559	2.022	1.971	0.690	0.532	0.546	3994.630
1.224	1.856	2.431	2.377	0.659	0.504	0.515	4413.355
1.613	2.236	2.955	2.894	0.721	0.546	0.557	4928.785
1.861	2.655	3.533	3.475	0.701	0.527	0.536	5439.824
2.164	3.228	4.323	4.267	0.670	0.501	0.507	6081.871
2.596	3.537	4.751	4.675	0.734	0.546	0.555	6443.145
2.984	4.042	5.447	5.364	0.738	0.548	0.556	6971.516
3.377	4.433	5.986	5.895	0.762	0.564	0.573	7377.004
3.917	4.878	6.598	6.478	0.803	0.594	0.605	7837.457
4.406	5.556	7.528	7.388	0.793	0.585	0.596	8467.820
4.921	5.885	7.980	7.810	0.836	0.617	0.630	8805.469
5.778	6.245	8.474	8.238	0.925	0.682	0.701	9213.082
6.415	6.635	9.009	8.747	0.967	0.712	0.733	9606.863
7.196	7.256	9.857	9.555	0.992	0.730	0.753	10187.480
8.078	7.288	9.902	9.552	1.108	0.816	0.846	10342.371
8.910	7.626	10.362	9.981	1.168	0.860	0.893	10712.969
9.695	8.220	11.171	10.753	1.179	0.868	0.907	11259.020
10.577	8.696	11.817	11.395	1.216	0.895	0.926	11725.633
11.408	8.929	12.133	11.701	1.278	0.940	0.975	12011.633
12.485	9.074	12.330	11.895	1.376	1.013	1.050	12269.215
13.316	9.564	12.993	12.563	1.392	1.025	1.060	12729.590